

Supporting Information

Based-assisted synthesis of 4-pyridinate gold(I)metallaligands and study of their participation in Self-Assembly reactions.

Montserrat Ferrer,^{a,b*} Albert Gutiérrez,^a Manuel Martínez,^{a,b} Cristiana Da Silva,^{c,d} Adelino V. G. Netto,^c Laura Rodríguez,^{a,b} Guillermo Romo-Islas,^{a,b} Fangfang Pan^e and Kari Rissanen^e

^a*Departament de Química Inorgànica i Orgànica, Secció de Química Inorgànica. Universitat de Barcelona, c/ Martí i Franquès 1-11, 08028 Barcelona, Spain.*

^b*Institut de Nanociència i Nanotecnologia (IN²UB). Universitat de Barcelona, 08028 Barcelona, Spain*

^c*UNESP–Univ Estadual Paulista, Insititute of Chemistry, 14800-060 Araraquara, SP, Brazil.*

^d*Faculdade de Ciências Exatas e Tecnologia, Universidade Federal da Grande Dourados, UFGD, Departamento de Química, P.O. Box 364, 79804-970, Dourados, MS, Brazil.*

^e*Department of Chemistry, University of Jyväskylä, POB 35, 40014 Jyväskylä, Finland.*

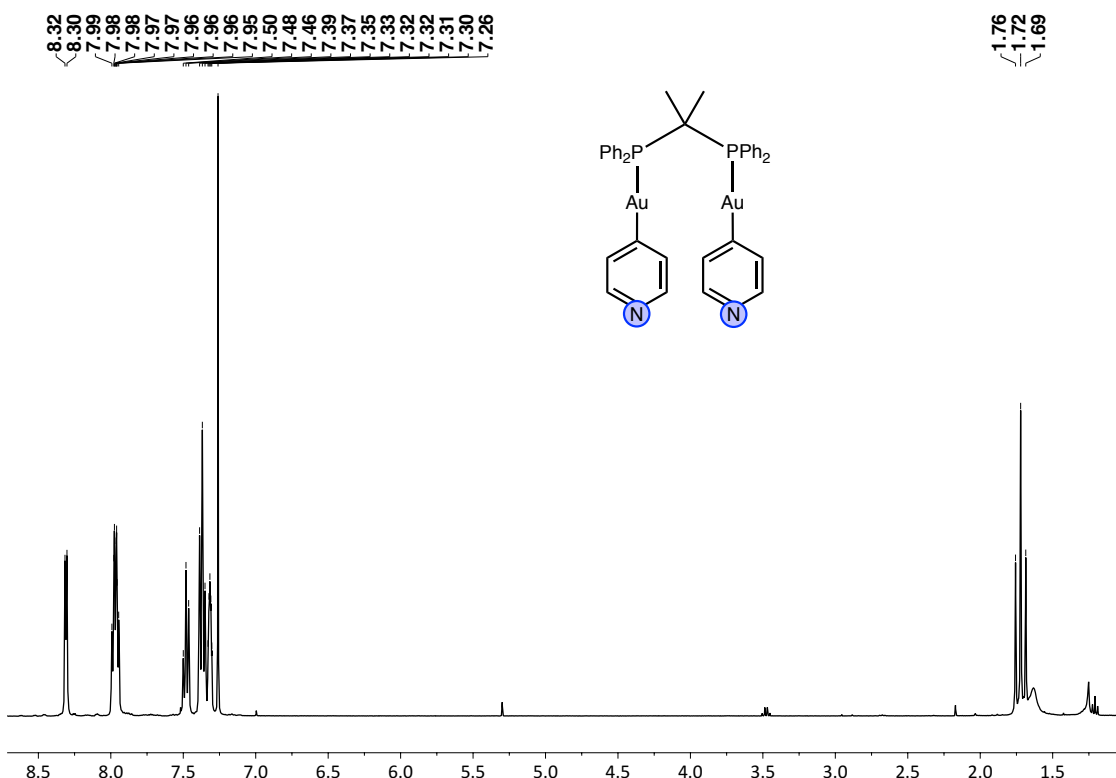


Figure S1. ^1H NMR of $[(\text{Au4-py})_2(\mu_2\text{-dppip})]$ (**1**) in CDCl_3 at 298 K.

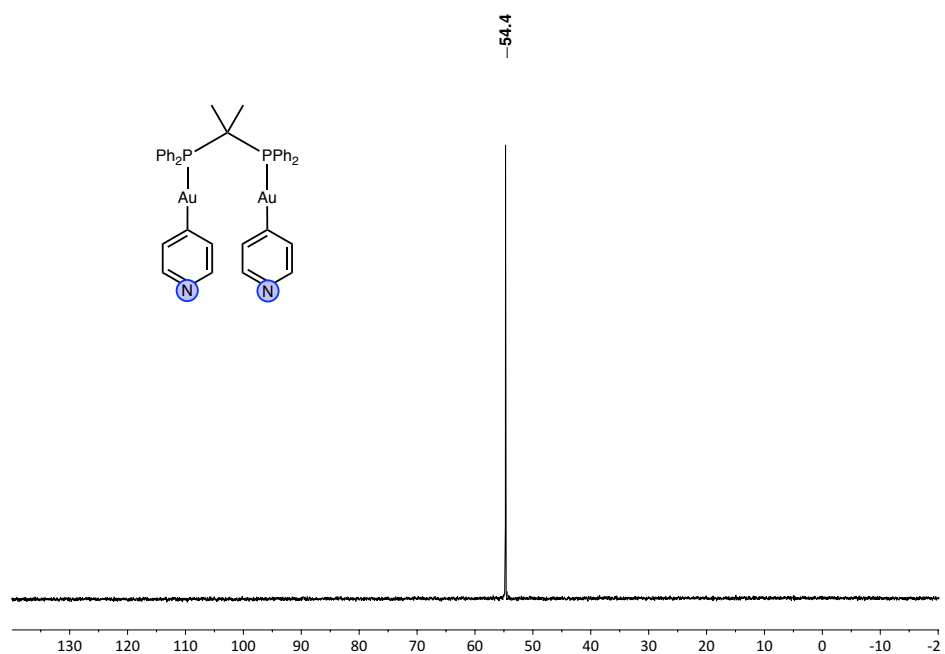


Figure S2. $^{31}\text{P}\{^1\text{H}\}$ NMR of $[(\text{Au4-py})_2(\mu_2\text{-dppip})]$ (**1**) in CDCl_3 at 298 K.

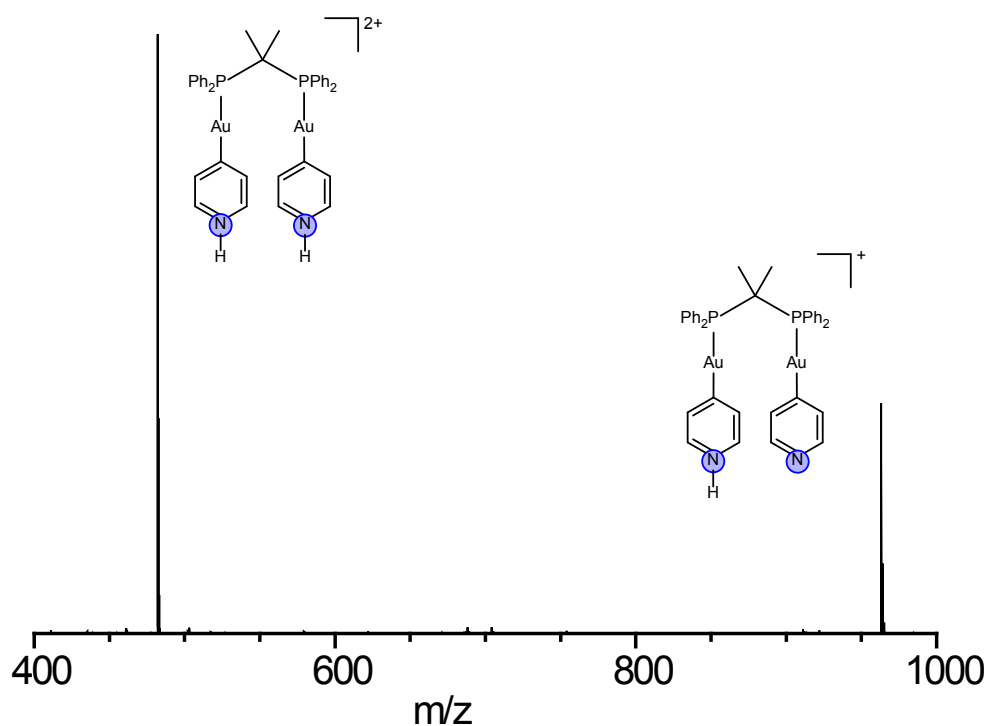


Figure S3. ESI(+) - HRMS spectrum of $[(\text{Au4-py})_2(\mu_2\text{-dppip})]$ (**1**).

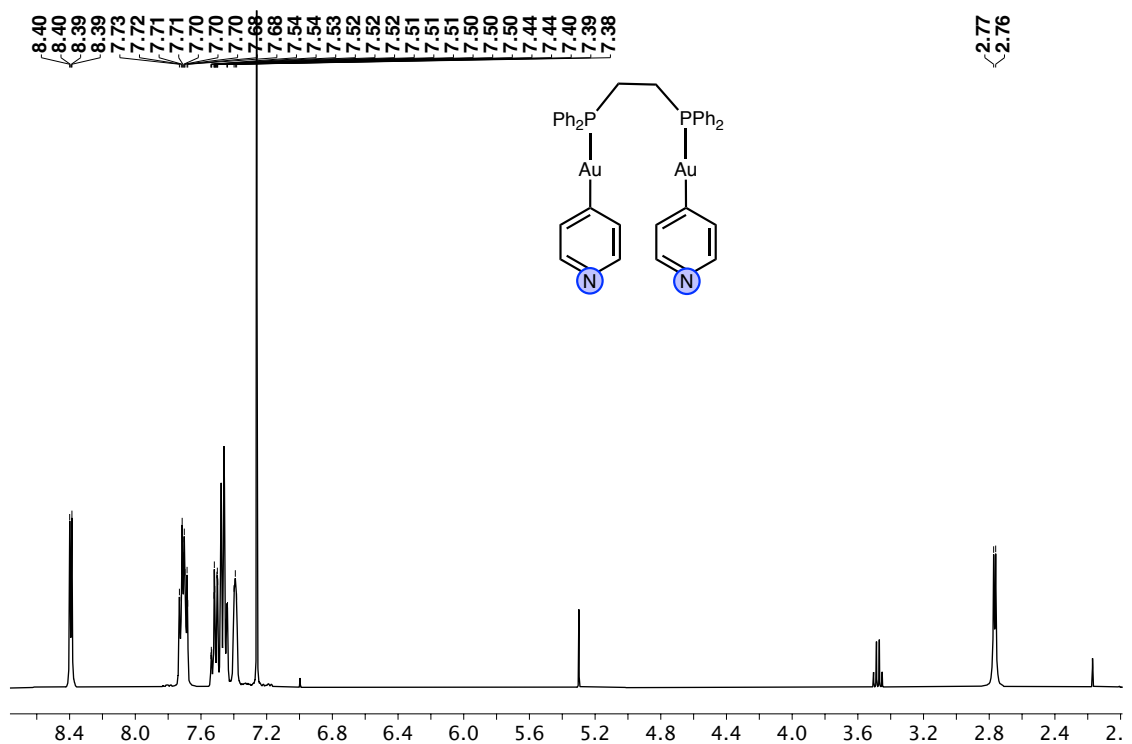


Figure S4. ¹H NMR of $[(\text{Au4-py})_2(\mu_2\text{-dppe})]$ (**2**) in CDCl₃ at 298 K.

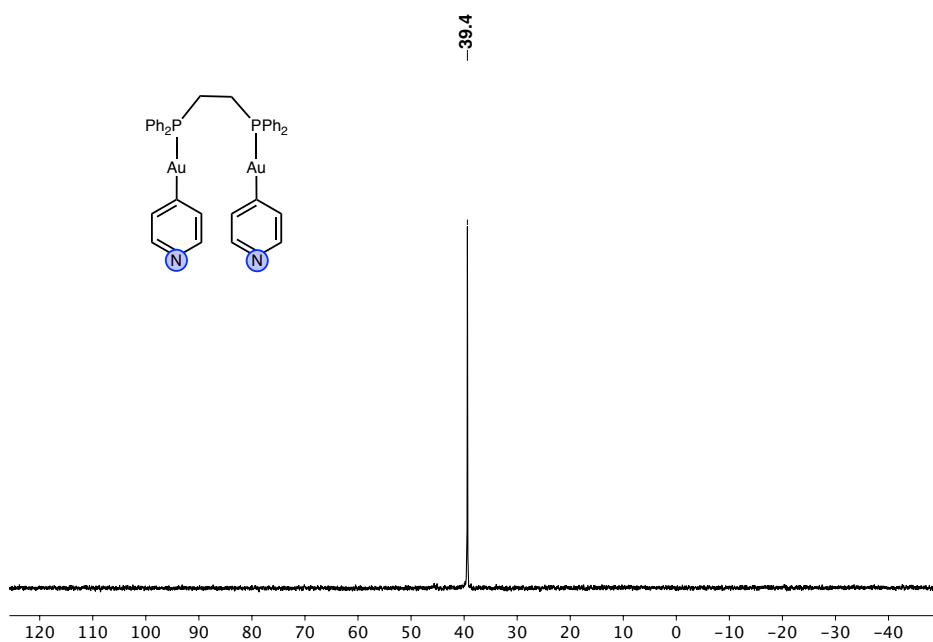


Figure S5. $^{31}\text{P}\{\text{H}\}$ NMR $[(\text{Au4-py})_2(\mu_2\text{-dppe})]$ (**2**) in CDCl_3 at 298 K.

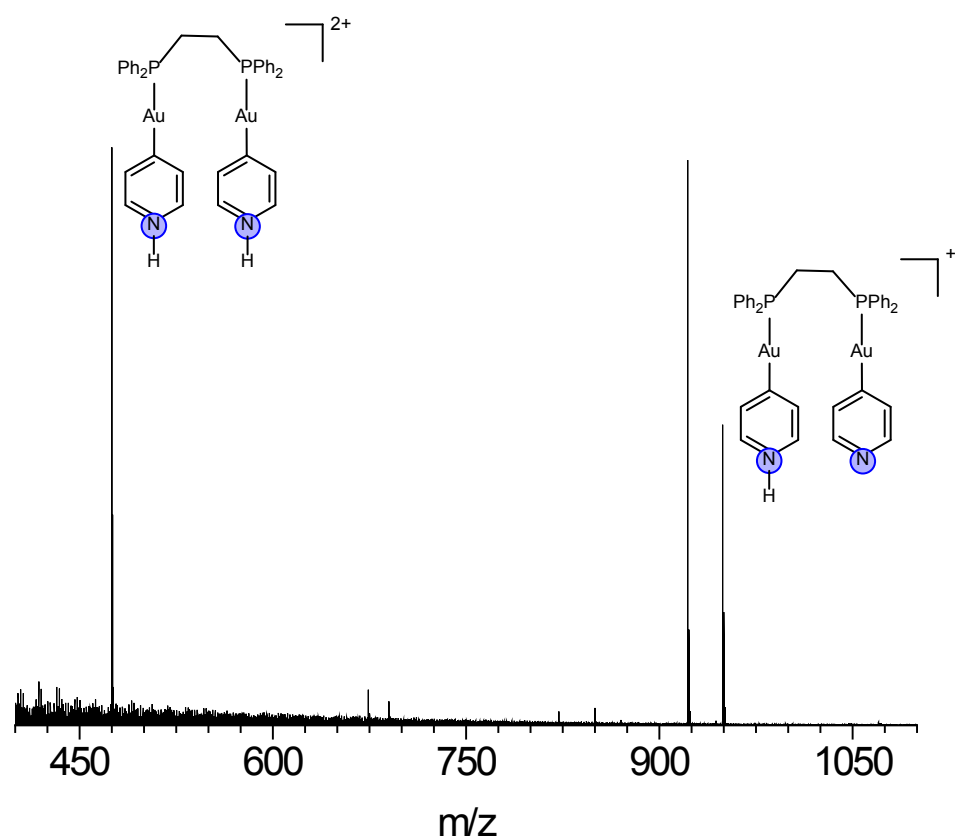


Figure S6. ESI(+)-HRMS spectrum of $[(\text{Au4-py})_2(\mu_2\text{-dppe})]$ (**2**).

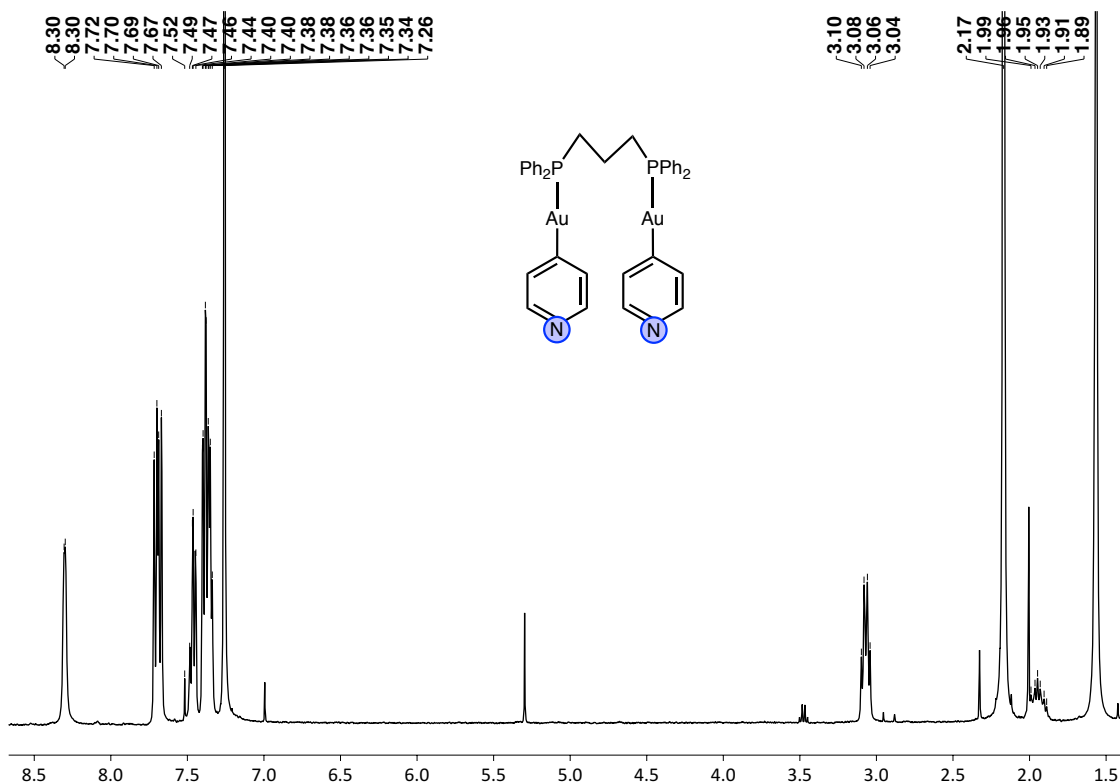


Figure S7. ^1H NMR of $[(\text{Au}_2\text{4-py})_2(\mu_2\text{-dPPP})]$ (**3**) in CDCl_3 at 298 K.

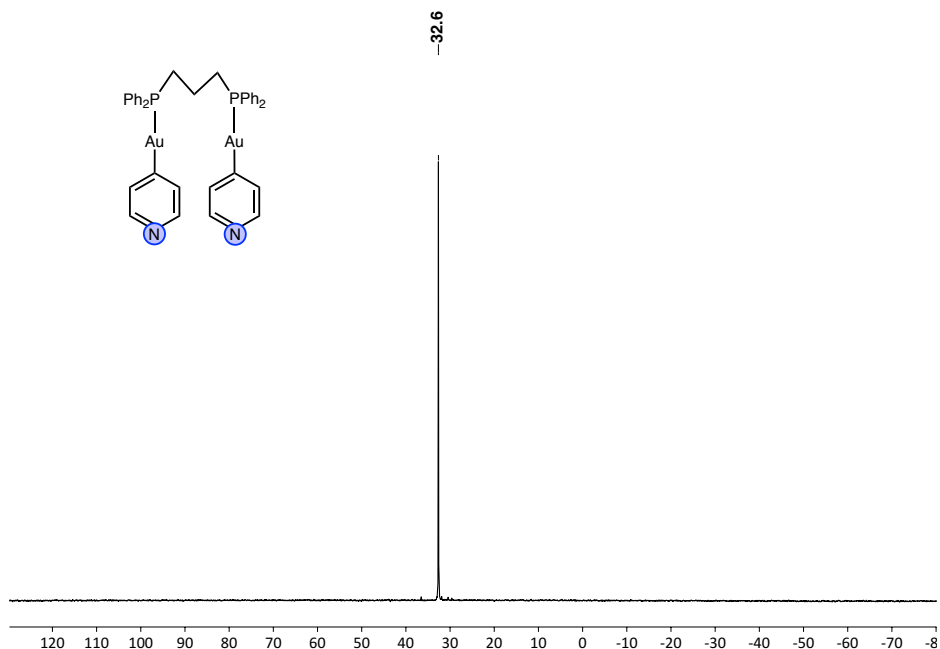


Figure S8. $^{31}\text{P}\{\text{H}\}$ NMR $[(\text{Au}_2\text{4-py})_2(\mu_2\text{-dPPP})]$ (**3**) in CDCl_3 at 298 K.

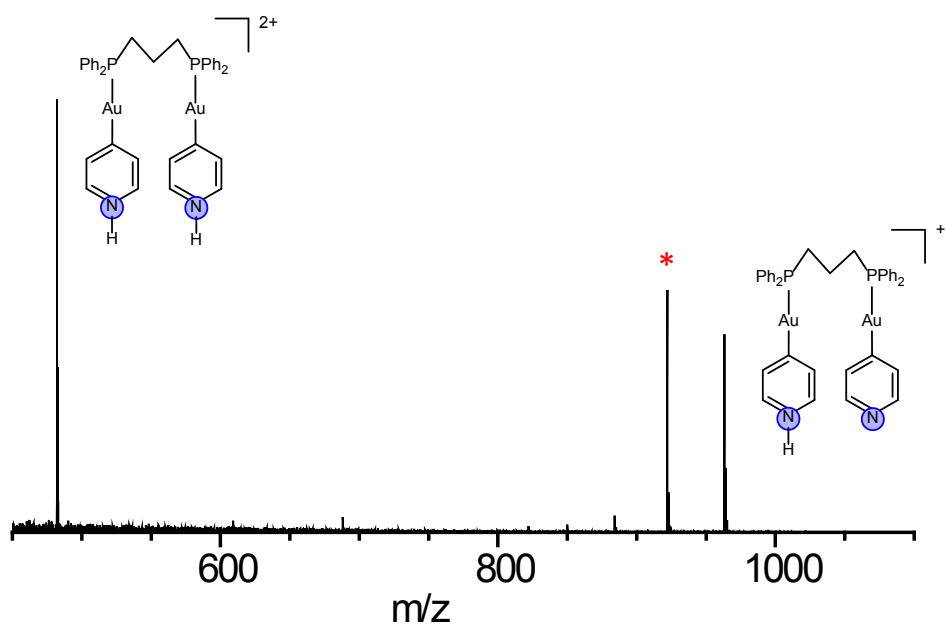


Figure S9. ESI(+) - HRMS spectrum of $[(\text{Au}4\text{-py})_2(\mu_2\text{-dppp})]$ (3). * Internal reference.

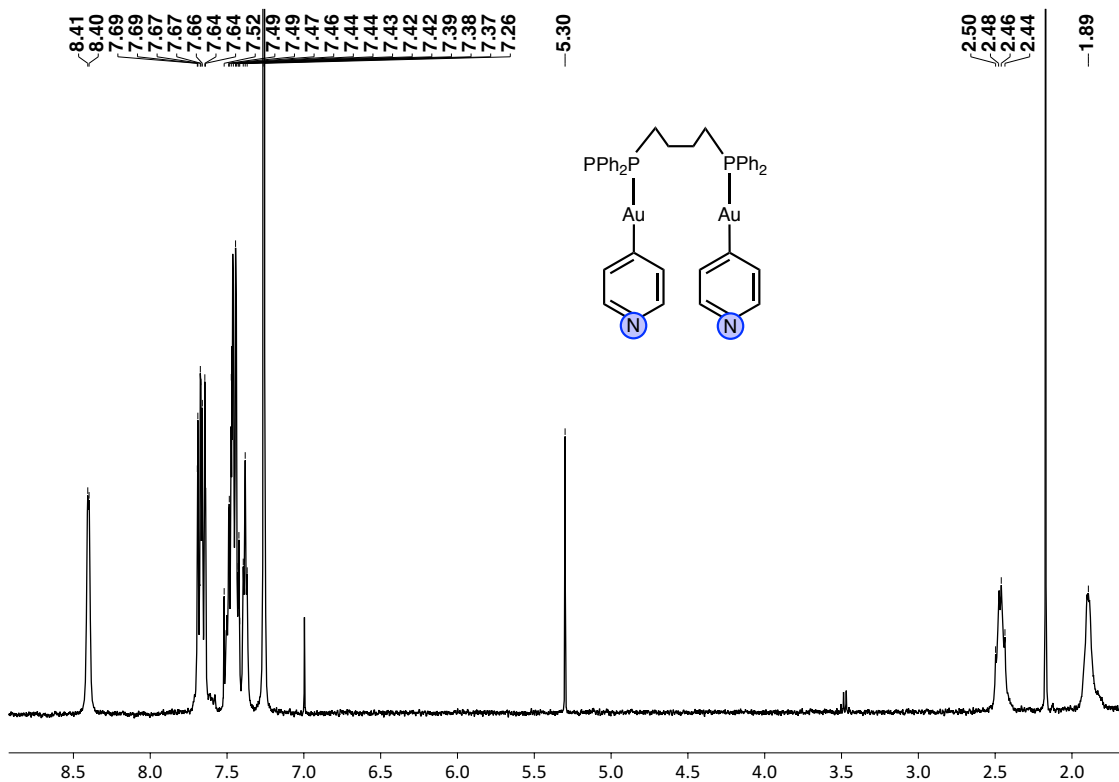


Figure S10. ^1H NMR of $[(\text{Au}4\text{-py})_2(\mu_2\text{-dppb})]$ (4) in CDCl_3 at 298 K.

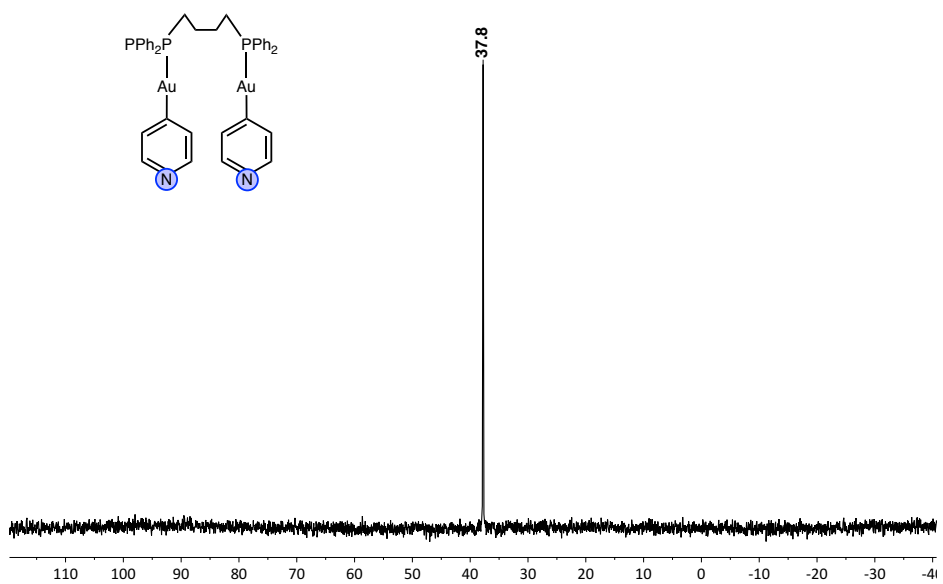


Figure S11. $^{31}\text{P}\{\text{H}\}$ NMR $[(\text{Au4-py})_2(\mu_2\text{-dppb})]$ (**4**) in CDCl_3 at 298 K.

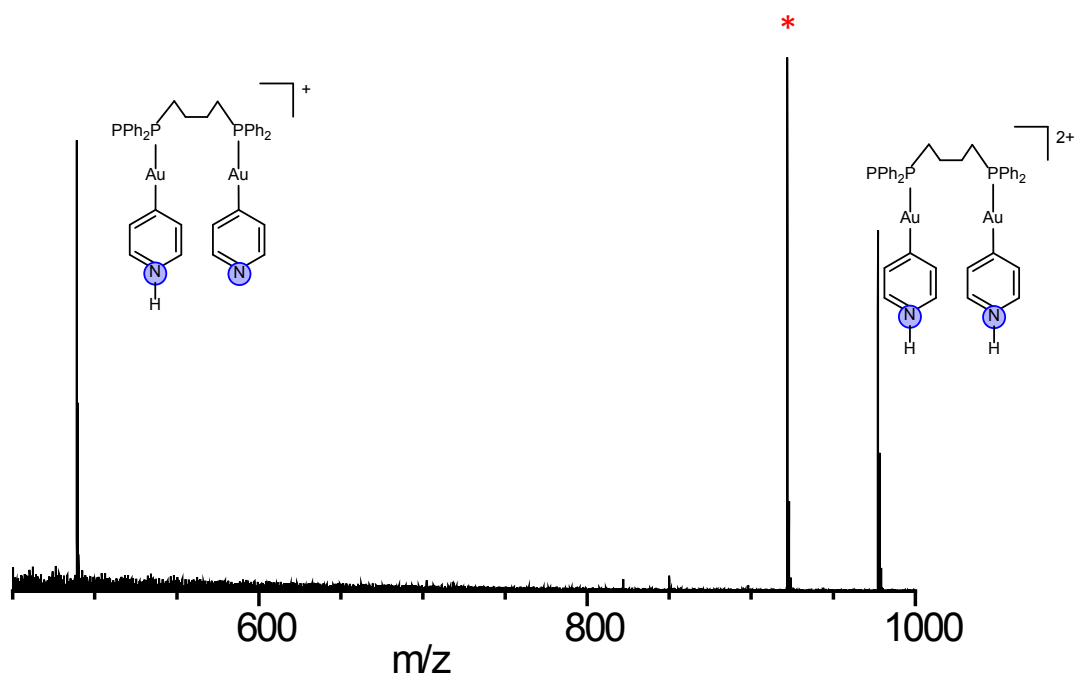


Figure S12. ESI(+) - HRMS spectrum of $[(\text{Au4-py})_2(\mu_2\text{-dppb})]$ (**4**). * Internal reference.

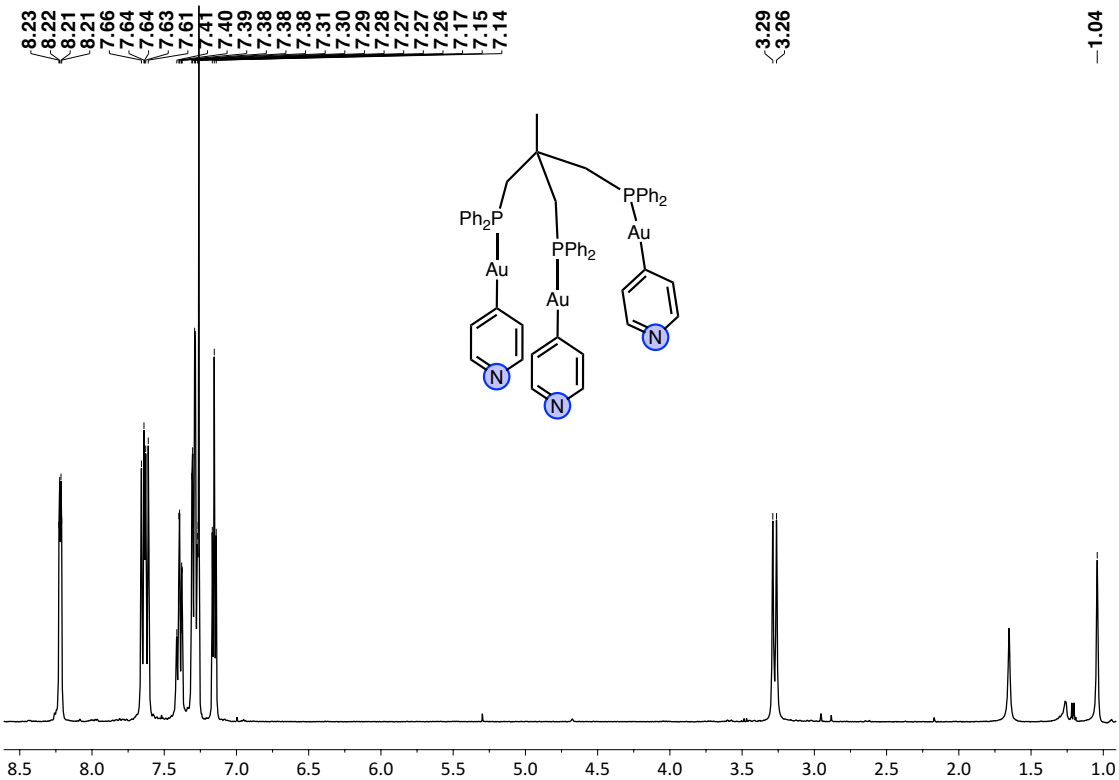


Figure S13. ^1H NMR of $[(\text{Au4-py})_3(\mu_3\text{-triphos})]$ (**5**) in CDCl_3 at 298 K.

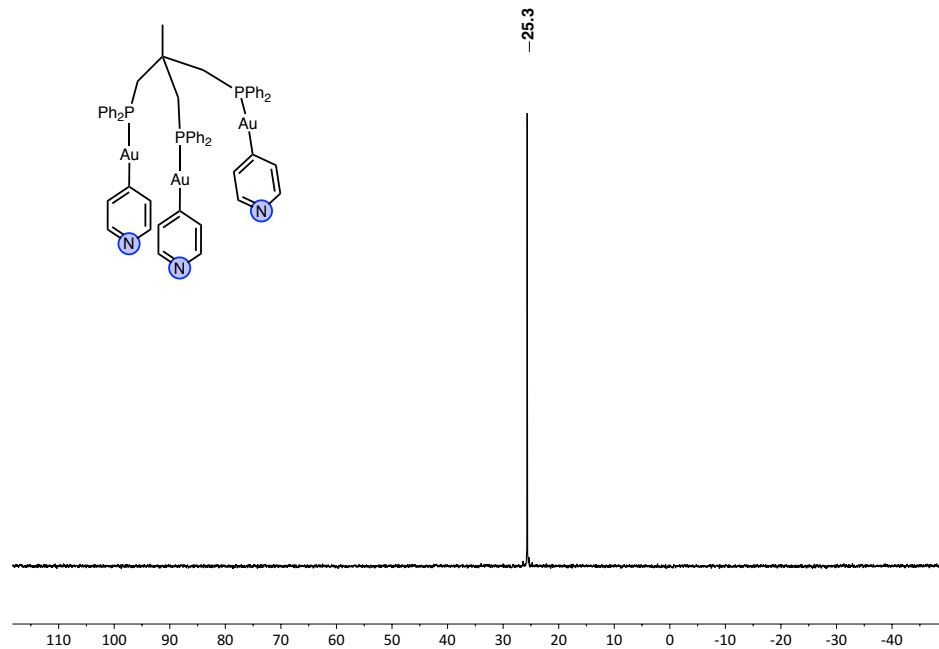


Figure S14. $^{31}\text{P}\{\text{H}\}$ NMR $[(\text{Au4-py})_3(\mu_3\text{-triphos})]$ (**5**) in CDCl_3 at 298 K.

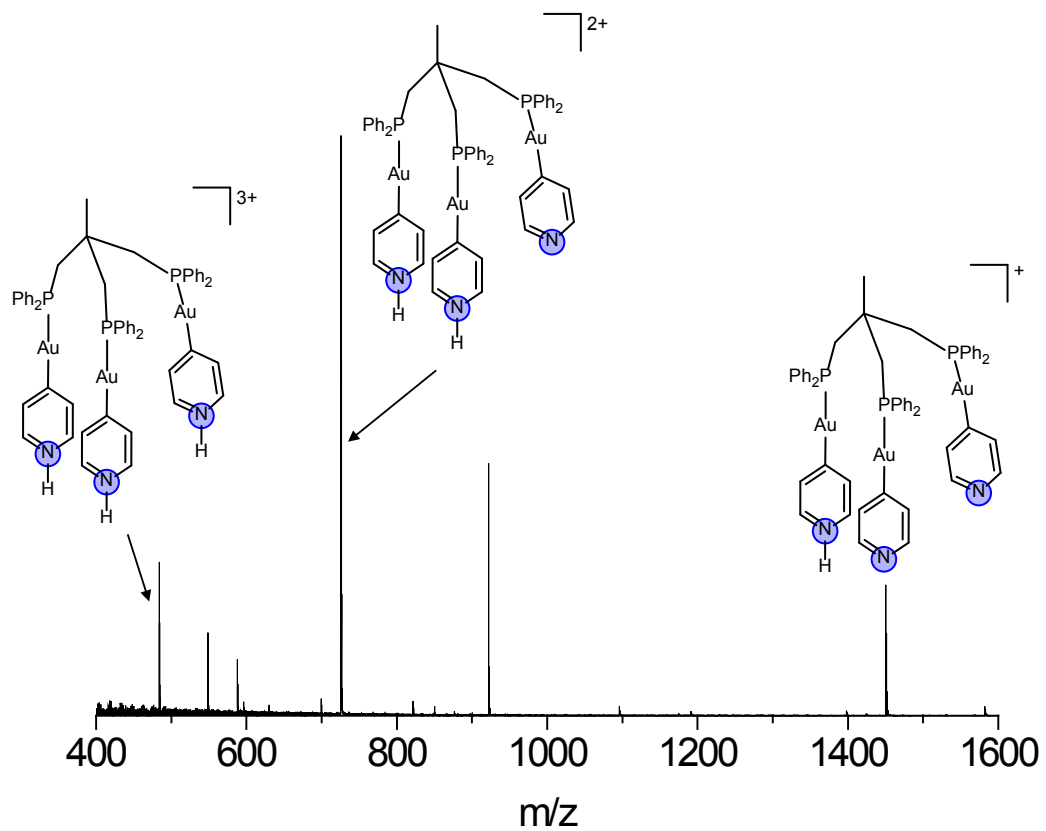


Figure S15. ESI(+) - HRMS spectrum of $[(\text{Au4-py})_3(\mu_3\text{-triphos})] (\mathbf{5})$.

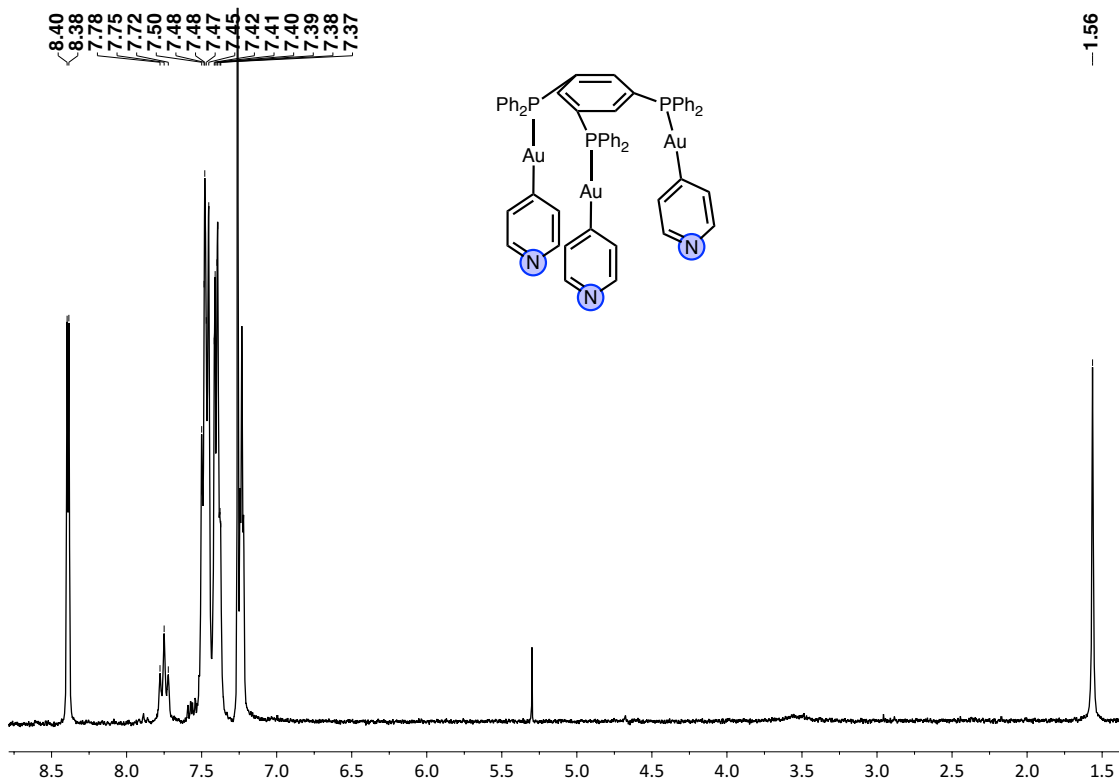


Figure S16. ^1H NMR of $[(\text{Au4-py})_3(\mu_3\text{-triphos})] (\mathbf{6})$ in CDCl_3 at 298 K.

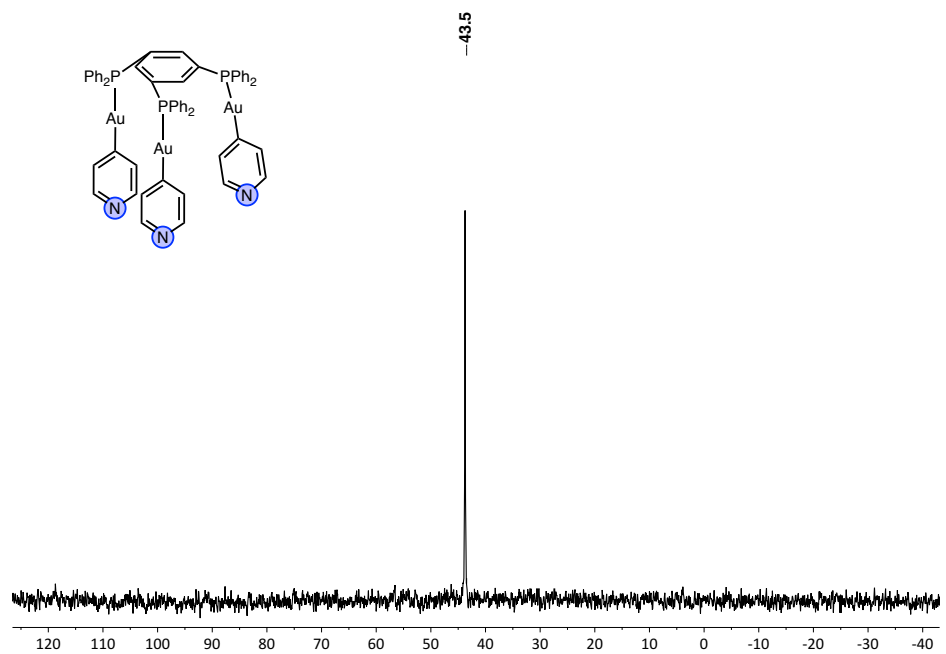


Figure S17. $^{31}\text{P}\{\text{H}\}$ NMR $[(\text{Au4-py})_3(\mu_3\text{-triphos})]$ (**6**) in CDCl_3 at 298 K.

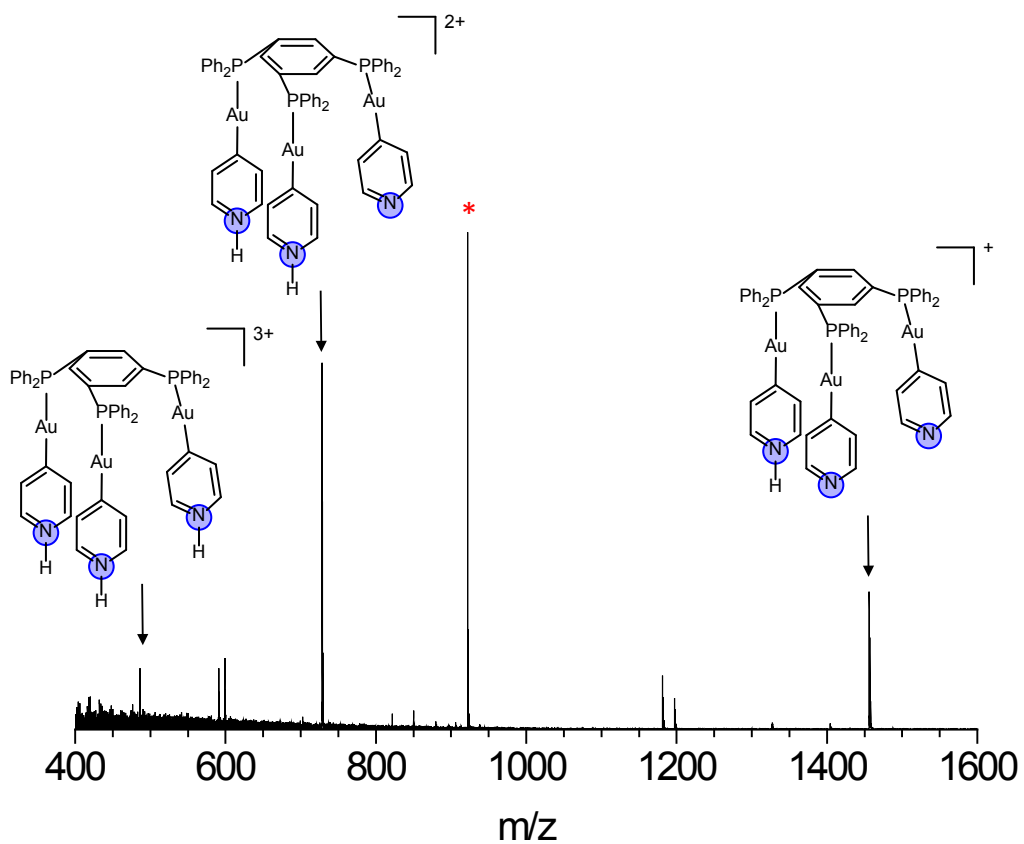


Figure S18. ESI(+)-HRMS spectrum of $[(\text{Au4-py})_3(\mu_3\text{-triphos})]$ (**6**). * Internal reference.

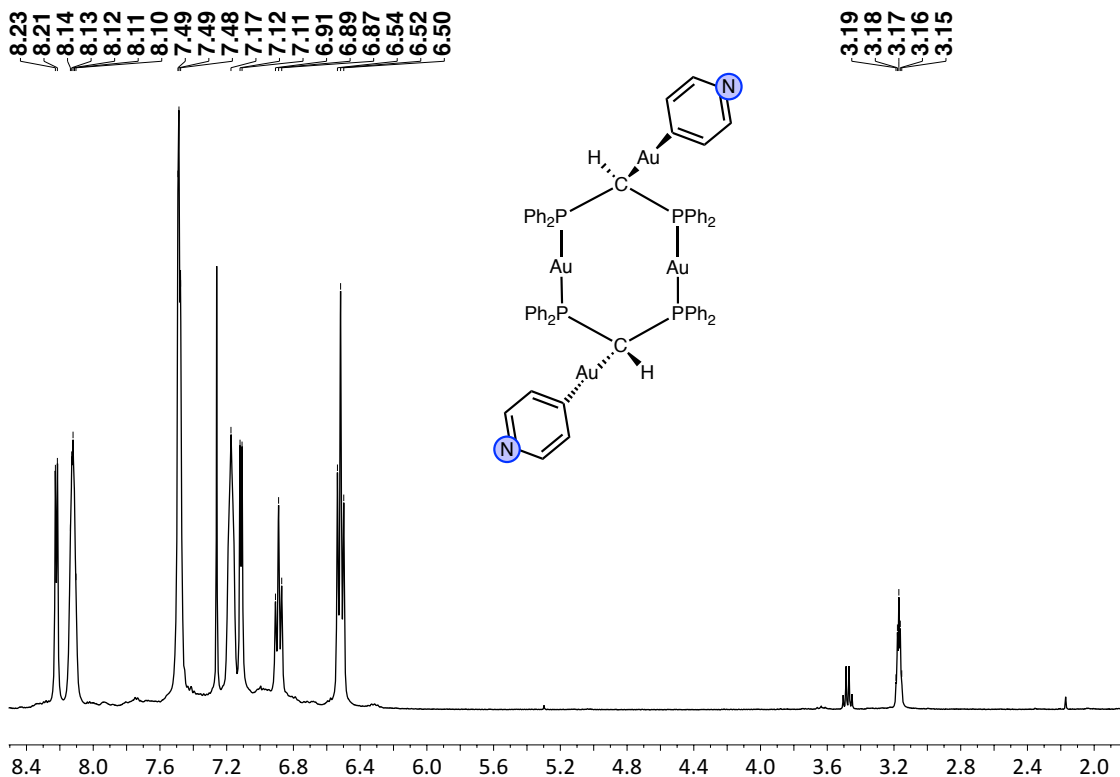


Figure S19. ^1H NMR of $[(\text{Au4-py})_2(\text{CH})_2(\mu_2\text{-Au}(\text{PPh}_2)_2)]$ (**I**) in CDCl_3 at 298 K.

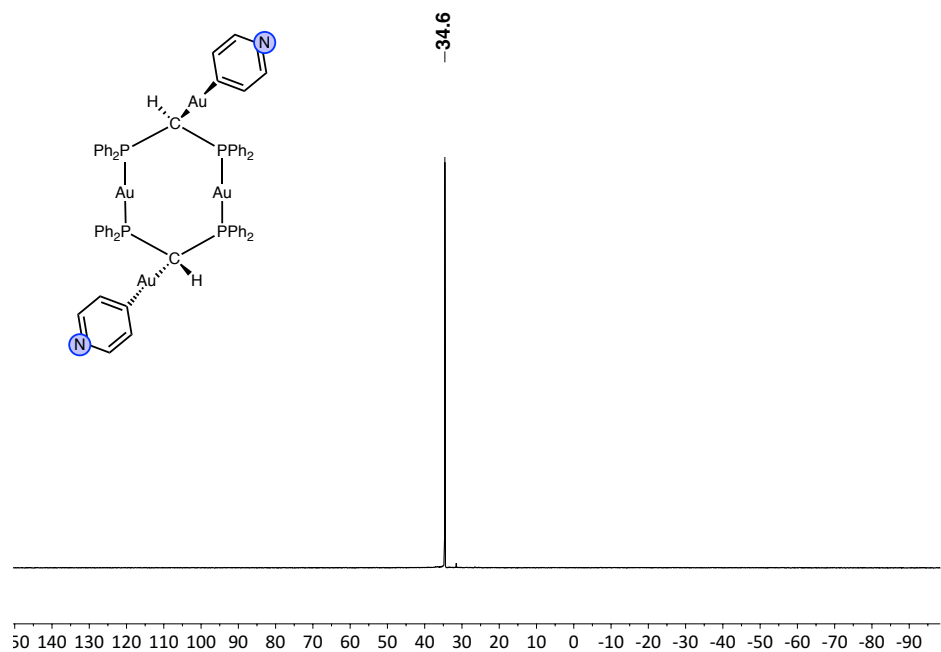


Figure S20. $^{31}\text{P}\{^1\text{H}\}$ NMR of $[(\text{Au4-py})_2(\text{CH})_2(\mu_2\text{-Au}(\text{PPh}_2)_2)]$ (**I**) in CDCl_3 at 298 K.

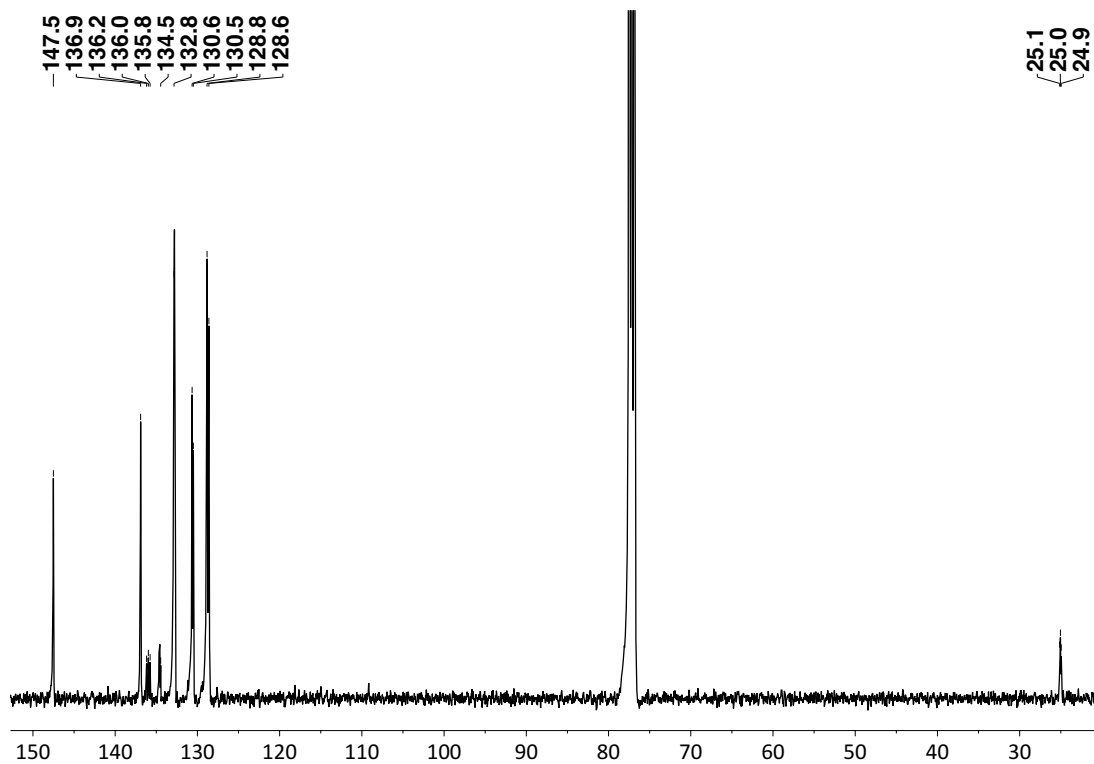


Figure S21. $^{13}\text{C}\{^1\text{H}\}$ NMR of $[(\text{Au4-py})_2(\text{CH})_2(\mu_2\text{-Au}(\text{PPh}_2)_2)]$ (**I**) in CDCl_3 at 298 K.

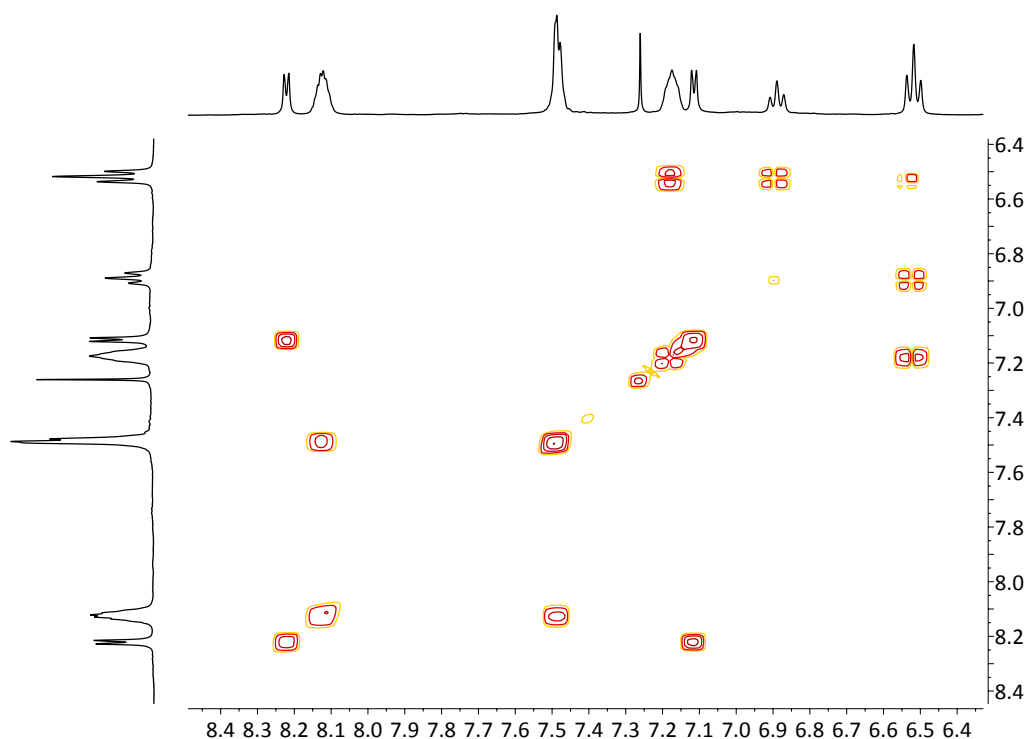


Figure S22. Partial ^1H - ^1H COSY NMR spectrum of $[(\text{Au4-py})_2(\text{CH})_2(\mu_2\text{-Au}(\text{PPh}_2)_2)]$ (**I**) at 298K.

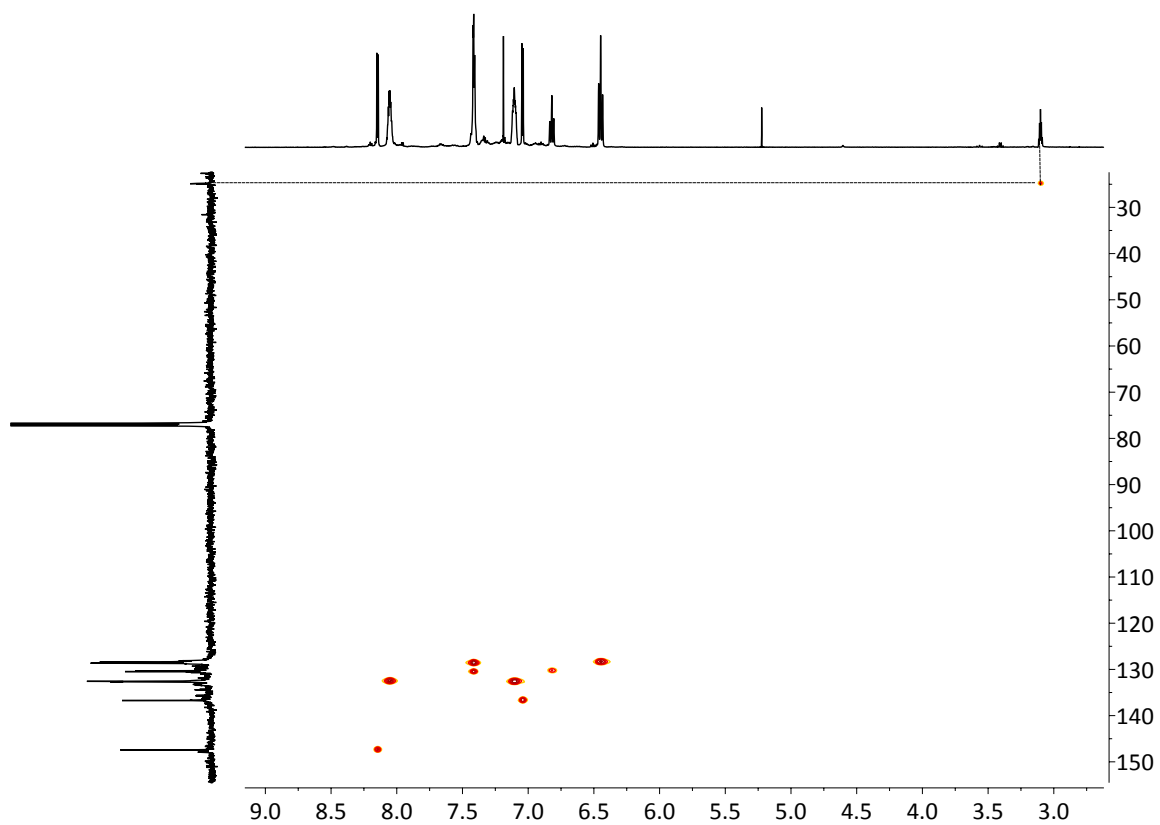


Figure S23. gHSQCAD NMR spectrum of $[\text{Au}_2(4\text{-py})_2(\text{CH})_2(\mu_2\text{-Au}(\text{PPh}_2)_2)]$ (**I**) at 298 K.

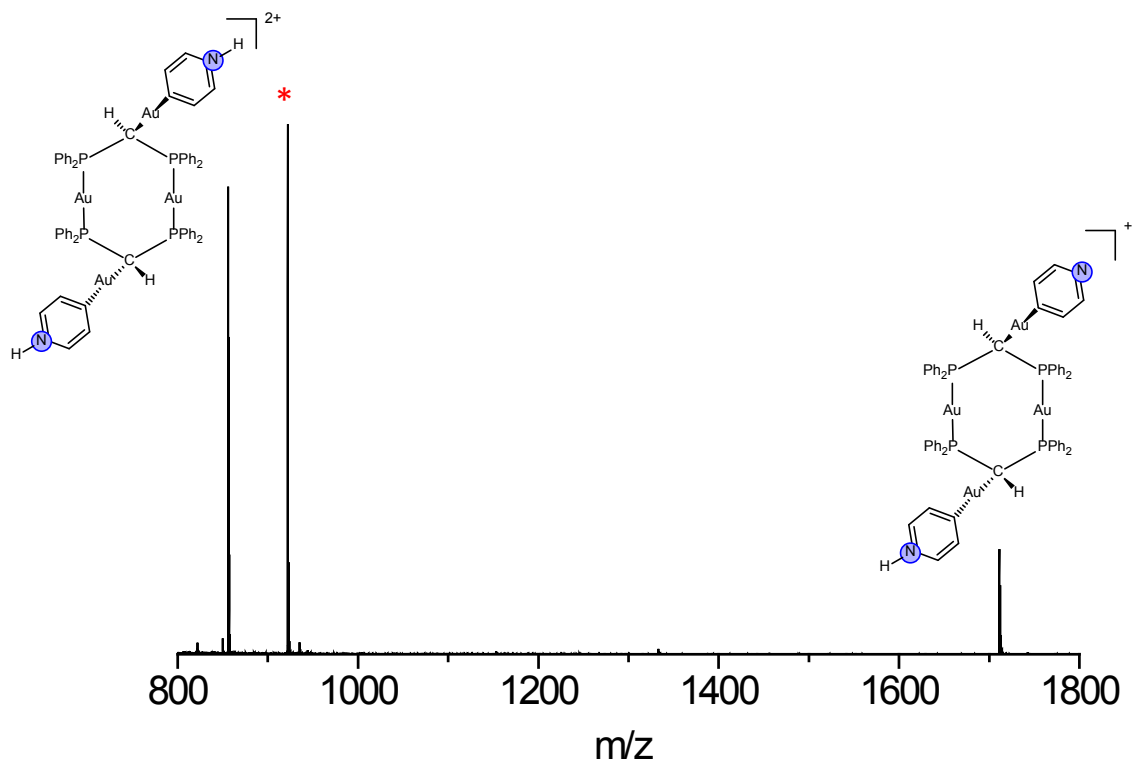


Figure S24. ESI(+) - HRMS spectrum of $[(\text{Au4-py})_2(\text{CH})_2(\mu_2\text{-Au}(\text{PPh}_2)_2)]$ (**I**). * Internal reference.

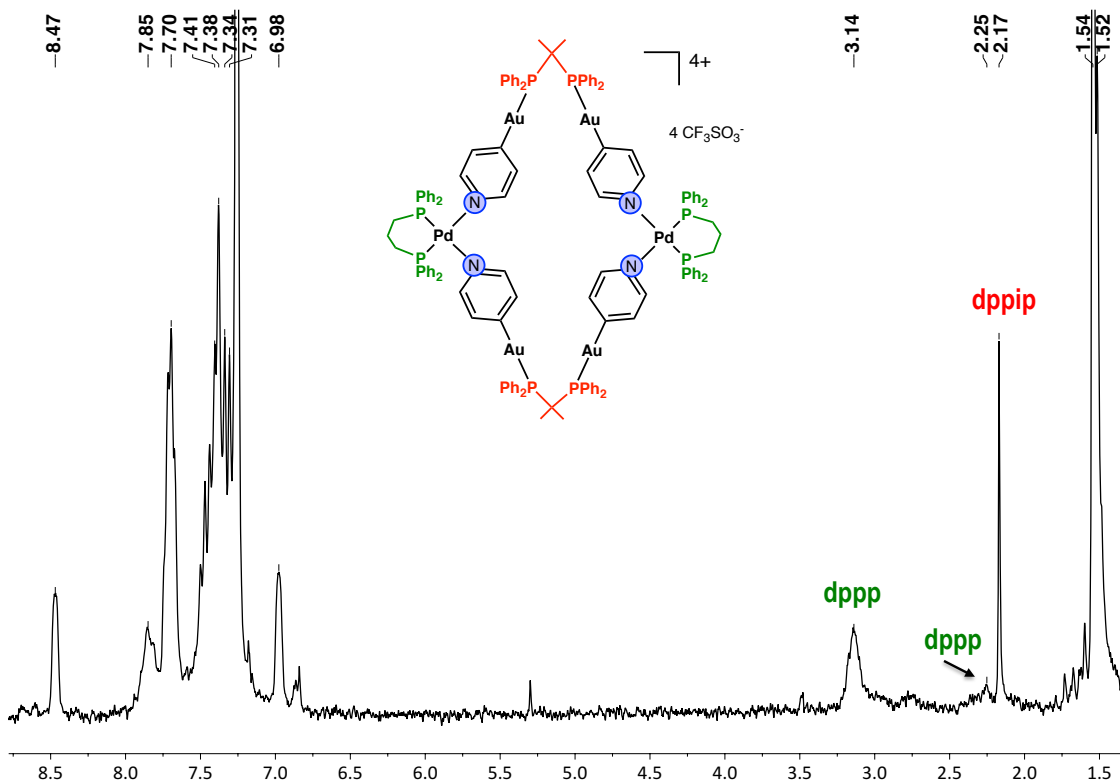


Figure S25. ^1H NMR of $\{(\text{Au4-py})_2(\mu_2\text{-dppip})\}_2\{\text{Pd(dppp)}\}_2(\text{CF}_3\text{SO}_3)_4$ (**1₂A₂**) in CDCl_3 at 298 K.

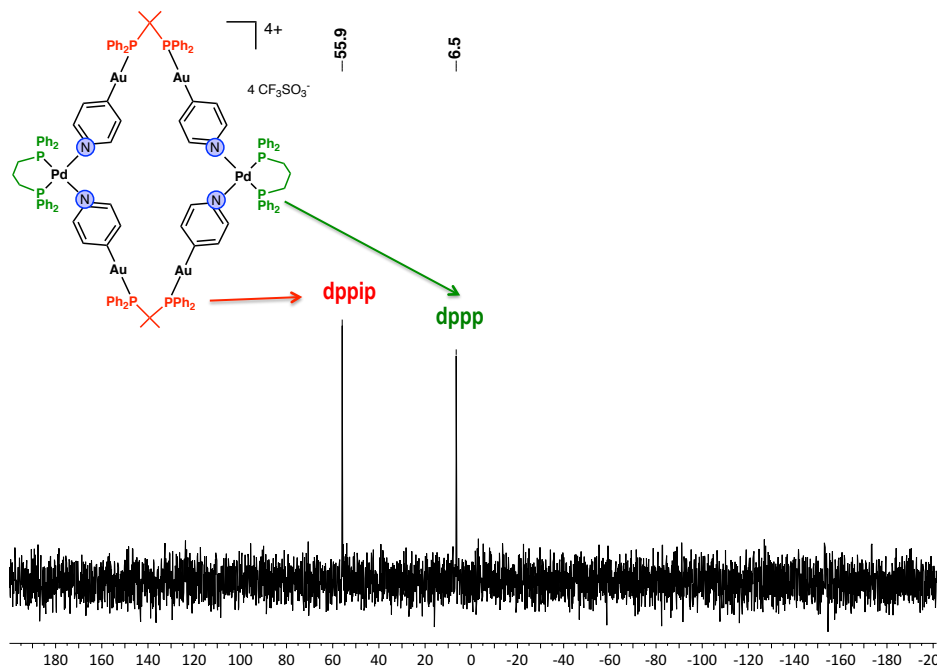


Figure S26. $^{31}\text{P}\{^1\text{H}\}$ NMR of $\{(\text{Au4-py})_2(\mu_2\text{-dppip})\}_2\{\text{Pd(dppp)}\}_2(\text{CF}_3\text{SO}_3)_4$ (**1₂A₂**) in CDCl_3 at 298K.

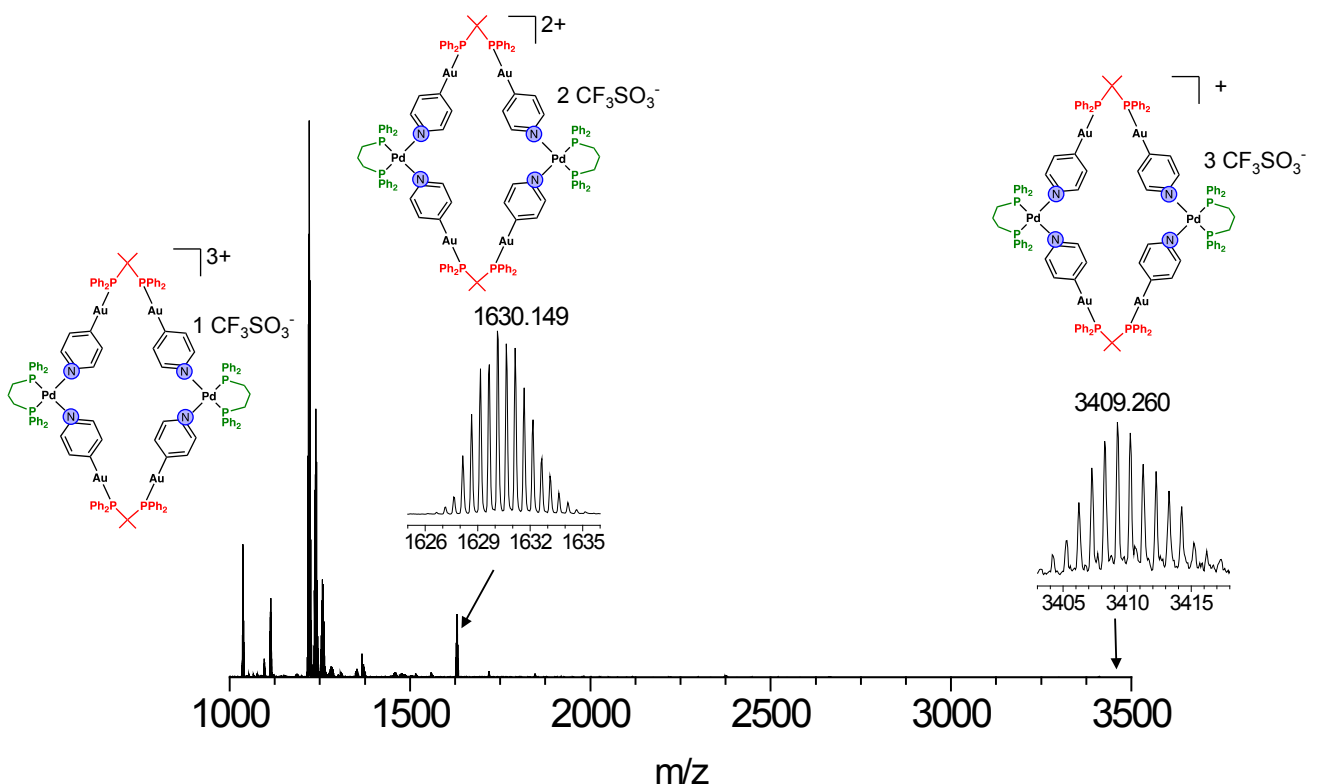


Figure S27. ESI(+)-HRMS spectrum of $\left[\{(\text{Au4-py})_2(\mu_2\text{-dppip})\}_2\{\text{Pd}(\text{dppp})\}_2\right](\text{CF}_3\text{SO}_3)_4$ ($\mathbf{1}_2\mathbf{A}_2$).

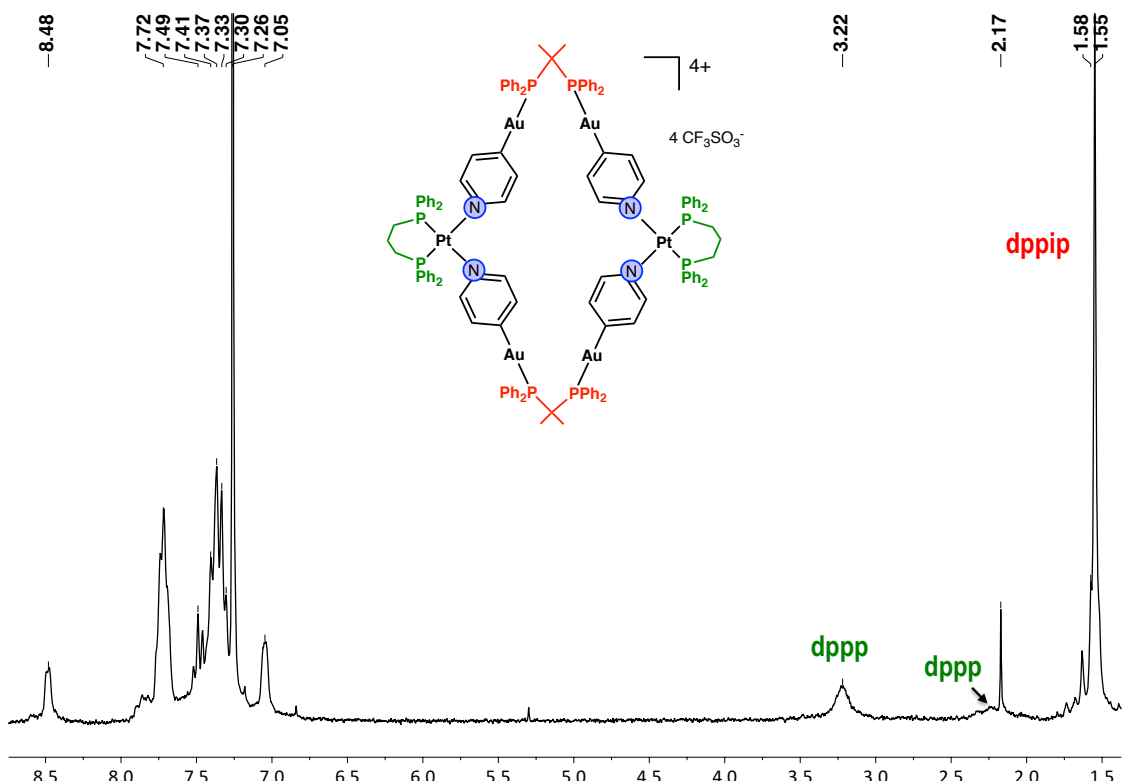


Figure S28. ^1H NMR of $\left[\{(\text{Au4-py})_2(\mu_2\text{-dppip})\}_2\{\text{Pt}(\text{dppp})\}_2\right](\text{CF}_3\text{SO}_3)_4$ ($\mathbf{1}_2\mathbf{B}_2$) in CDCl_3 at 298 K.

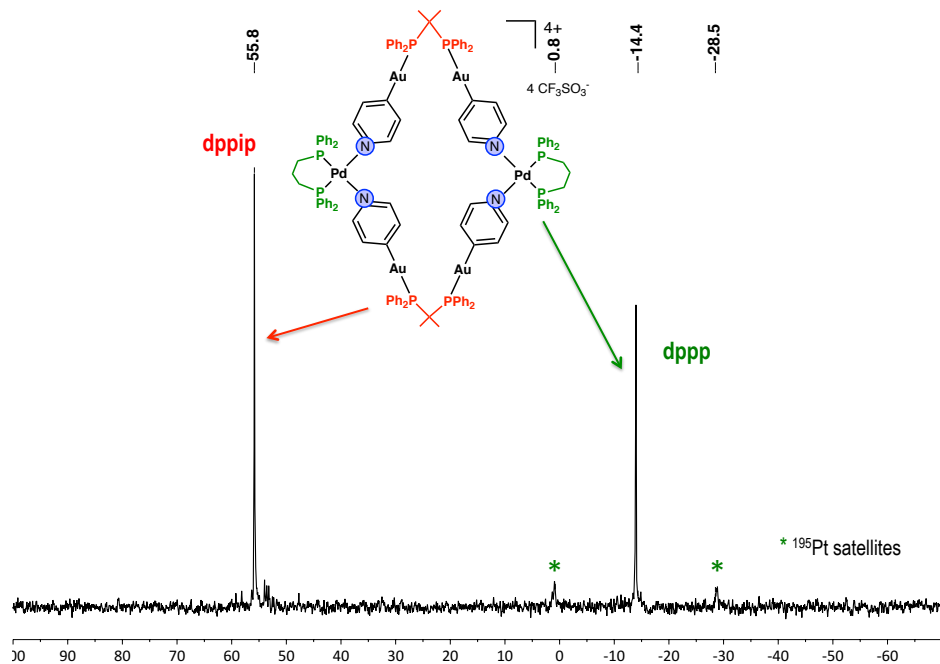


Figure S29. $^{31}\text{P}\{\text{H}\}$ NMR of $\{(\text{Au4-py})_2(\mu_2\text{-dppip})\}_2\{\text{Pt(dPPP)}\}_2](\text{CF}_3\text{SO}_3)_4$ (**1₂B₂**) in CDCl_3 at 298K.

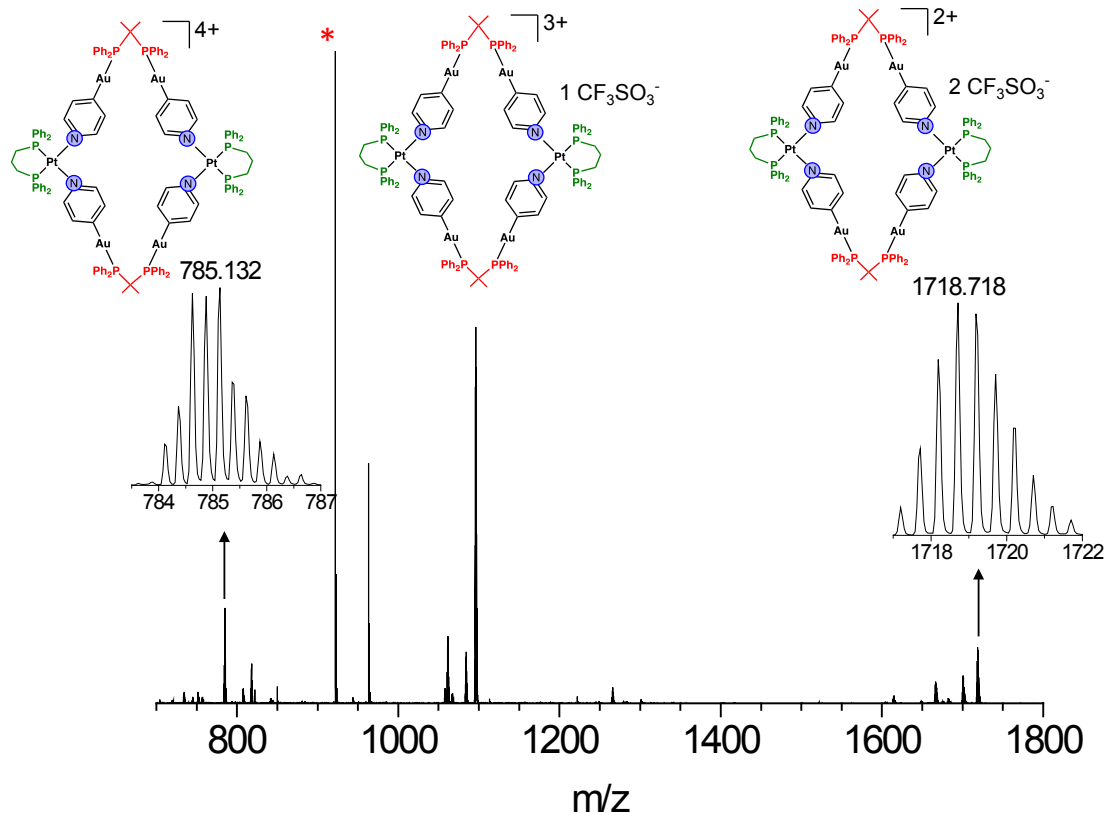


Figure S30. ESI(+)-HRMS spectrum of $\{(\text{Au4-py})_2(\mu_2\text{-dppip})\}_2\{\text{Pt(dPPP)}\}_2](\text{CF}_3\text{SO}_3)_4$ (**1₂B₂**).

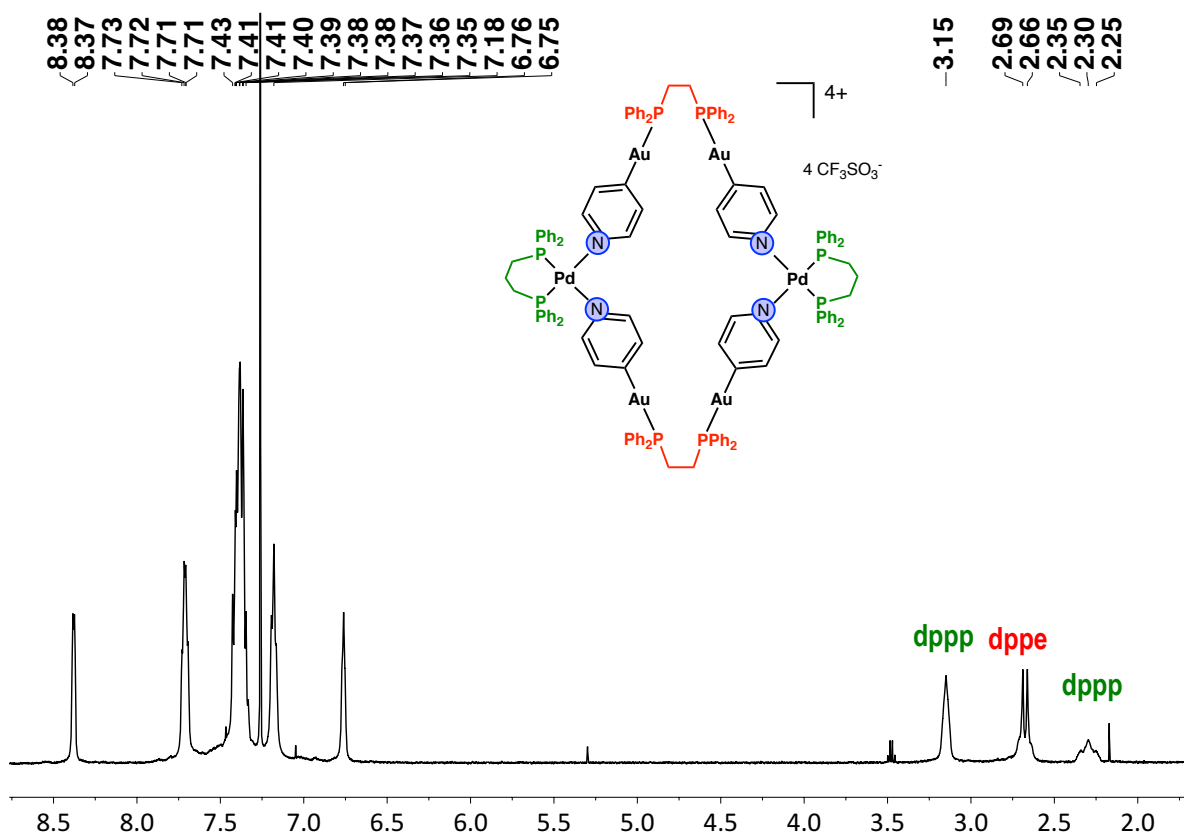


Figure S31. ^1H NMR of $\{(\text{Au4-py})_2(\mu_2\text{-dppe})\}_2\{\text{Pd(dPPP)}\}_2](\text{CF}_3\text{SO}_3)_4$ (**2A₂**) in CDCl_3 at 298 K.

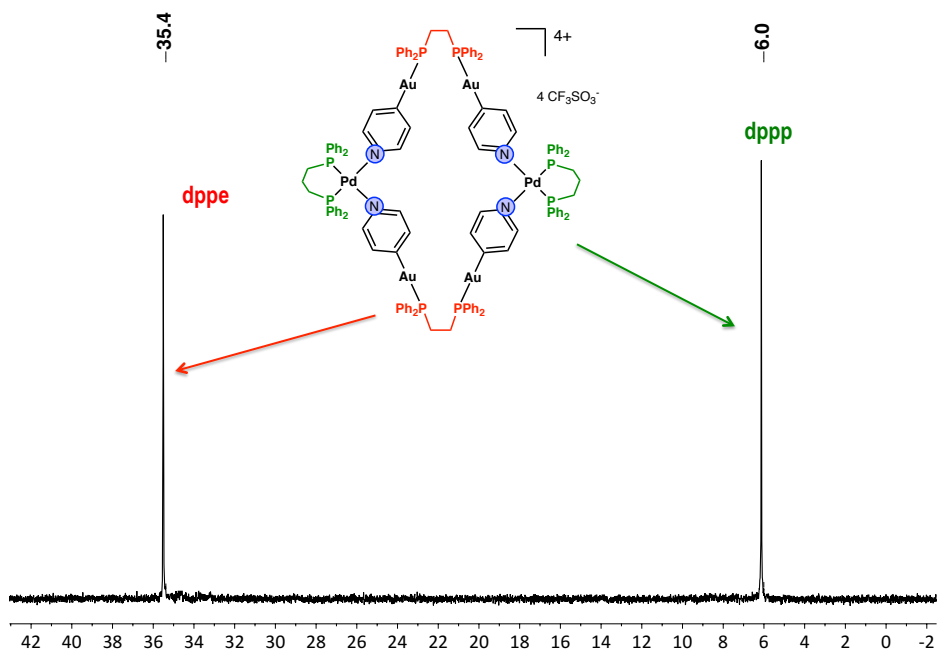


Figure S32. $^{31}\text{P}\{^1\text{H}\}$ NMR of $\{(\text{Au4-py})_2(\mu_2\text{-dppe})\}_2\{\text{Pd(dPPP)}\}_2](\text{CF}_3\text{SO}_3)_4$ (**2A₂**) in CDCl_3 at 298 K.

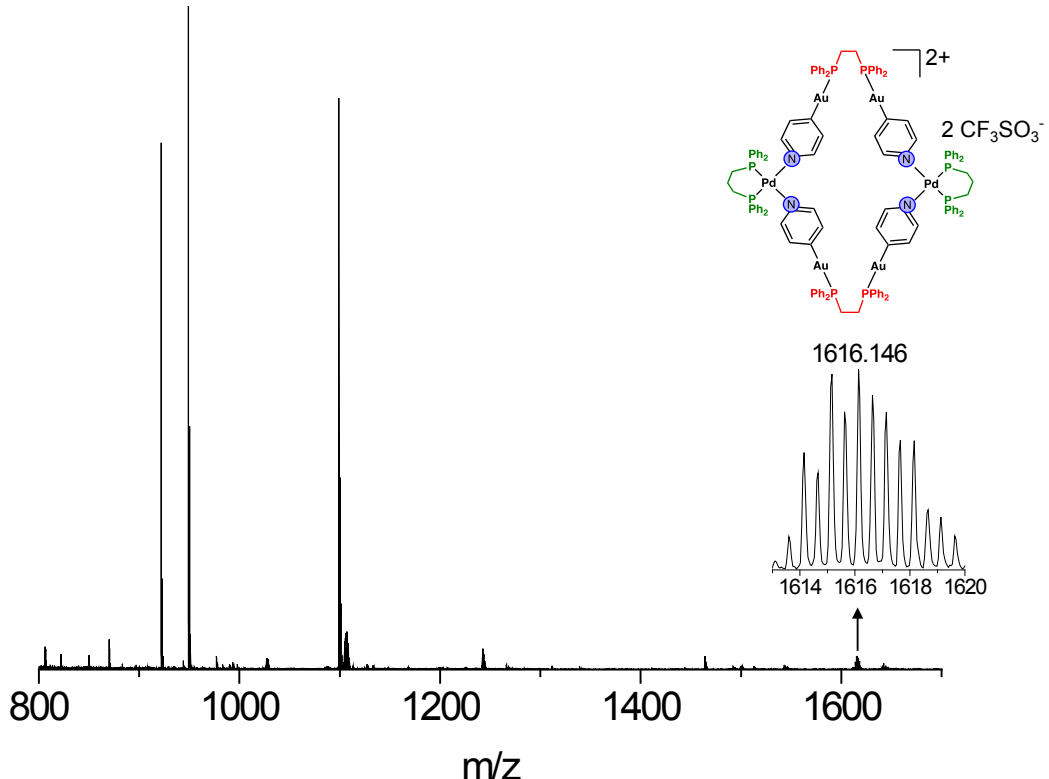


Figure S33. ESI(+) - HRMS spectrum of $\left[\left\{ (\text{Au}^{\text{4-py}})_2(\mu_2\text{-dppe}) \right\}_2 \left\{ \text{Pd}(\text{dPPP}) \right\}_2 \right] (\text{CF}_3\text{SO}_3)_4^{2+}$ (**2₂A₂**).

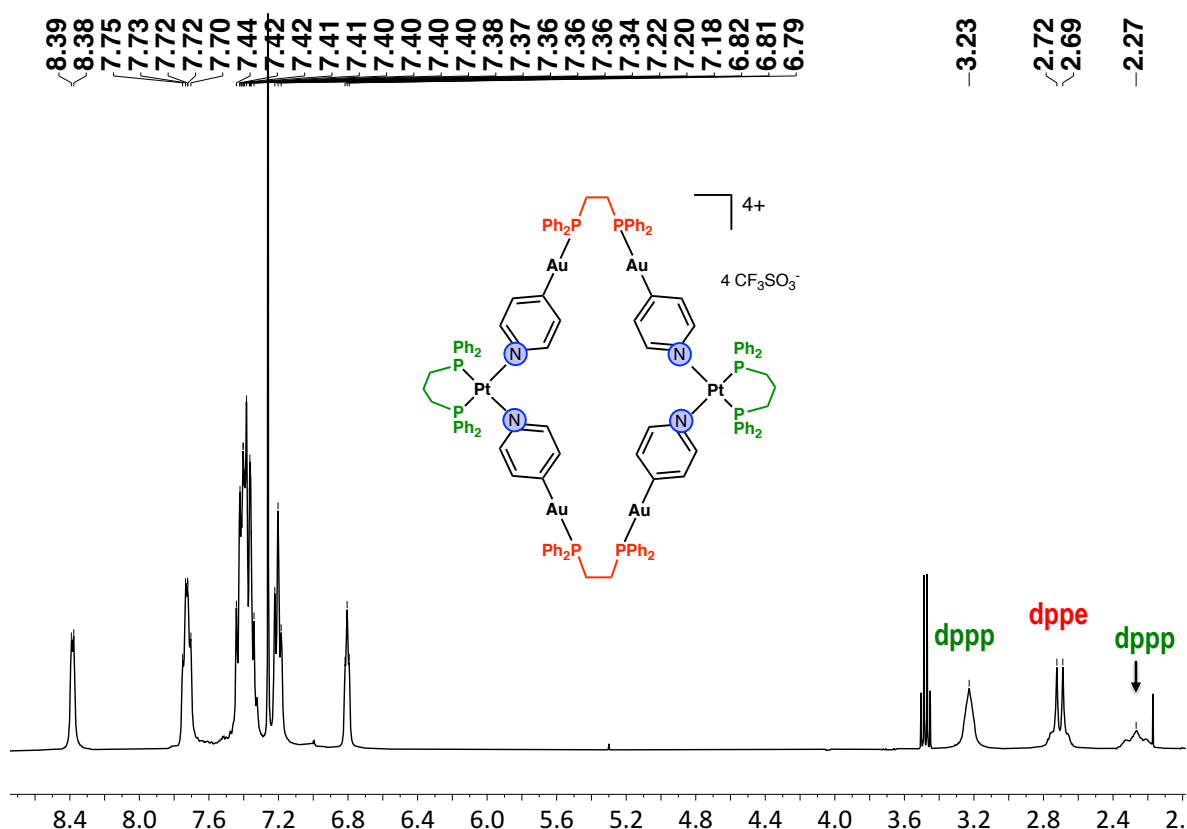


Figure S34. ${}^1\text{H}$ NMR of $\left[\left\{ (\text{Au}^{\text{4-py}})_2(\mu_2\text{-dppe}) \right\}_2 \left\{ \text{Pt}(\text{dPPP}) \right\}_2 \right] (\text{CF}_3\text{SO}_3)_4^{4+}$ (**2₂B₂**) in CDCl_3 at 298 K.

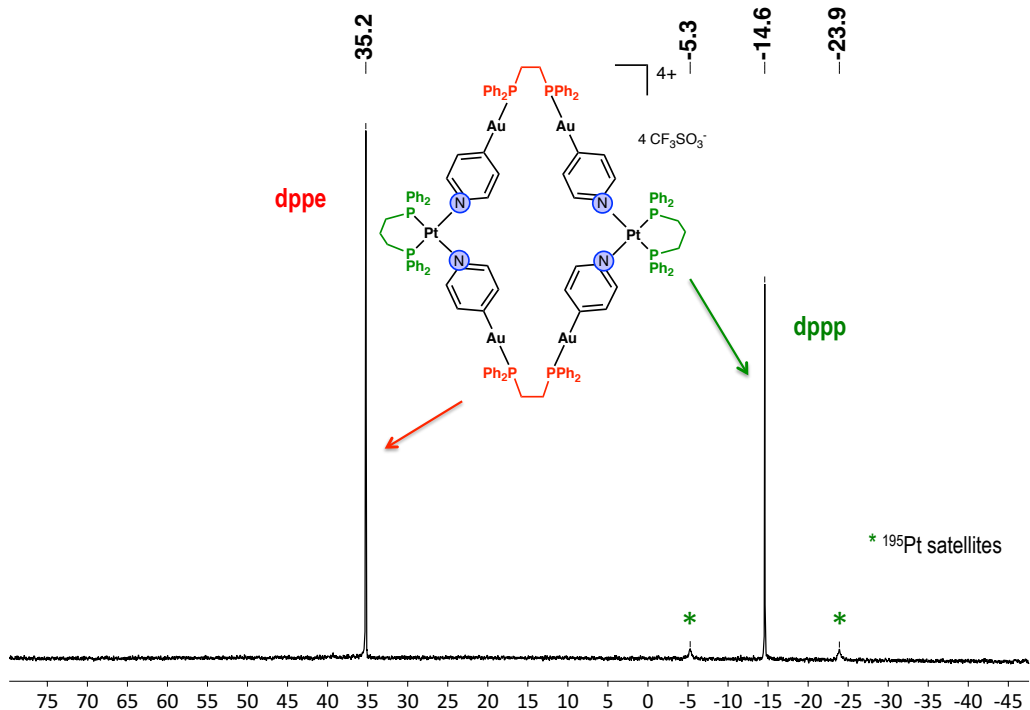


Figure S35. $^{31}\text{P}\{\text{H}\}$ NMR of $\{(\text{Au4-py})_2(\mu_2\text{-dppe})\}_2\{\text{Pt}(\text{dPPP})\}_2\}(\text{CF}_3\text{SO}_3)_4$ (**2₂B₂**) in CDCl_3 at 298 K.

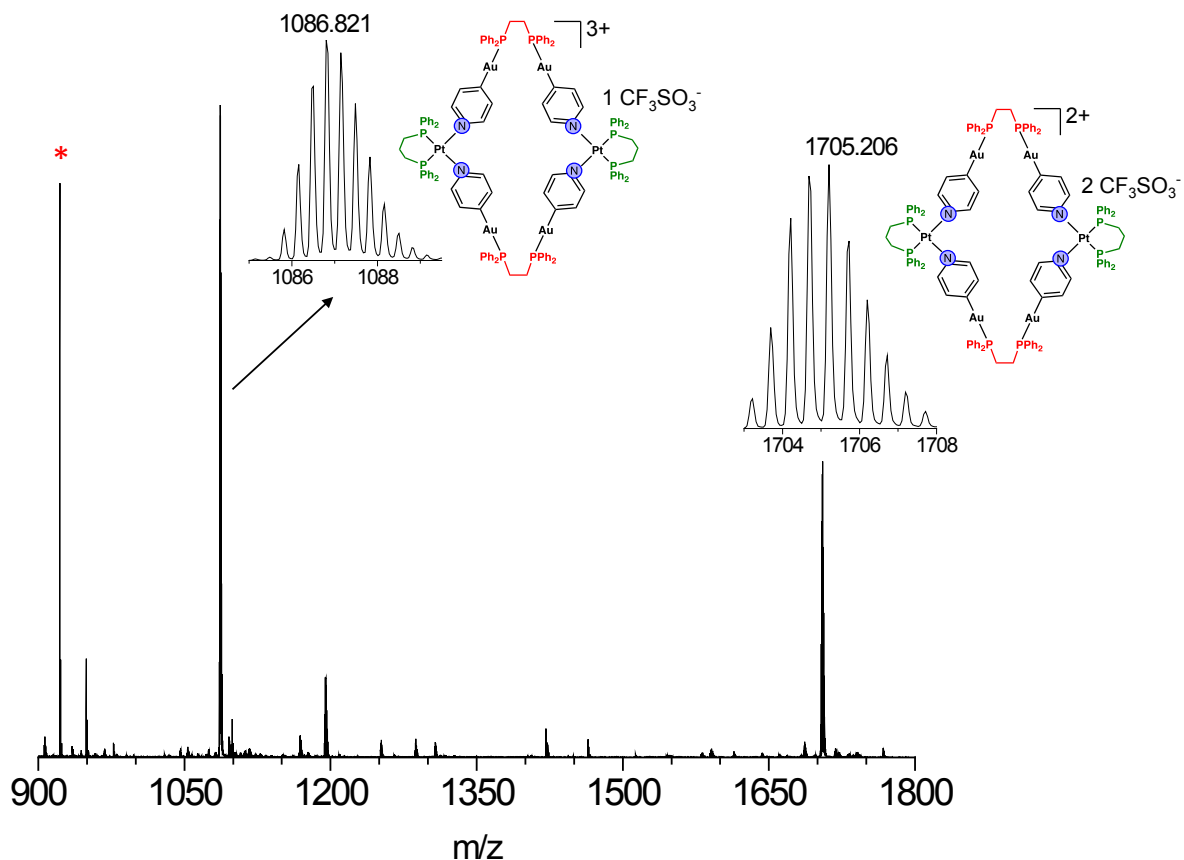


Figure S36. ESI(+)-HRMS spectrum of $\{(\text{Au4-py})_2(\mu_2\text{-dppe})\}_2\{\text{Pt}(\text{dPPP})\}_2\}(\text{CF}_3\text{SO}_3)_4$ (**2₂B₂**).

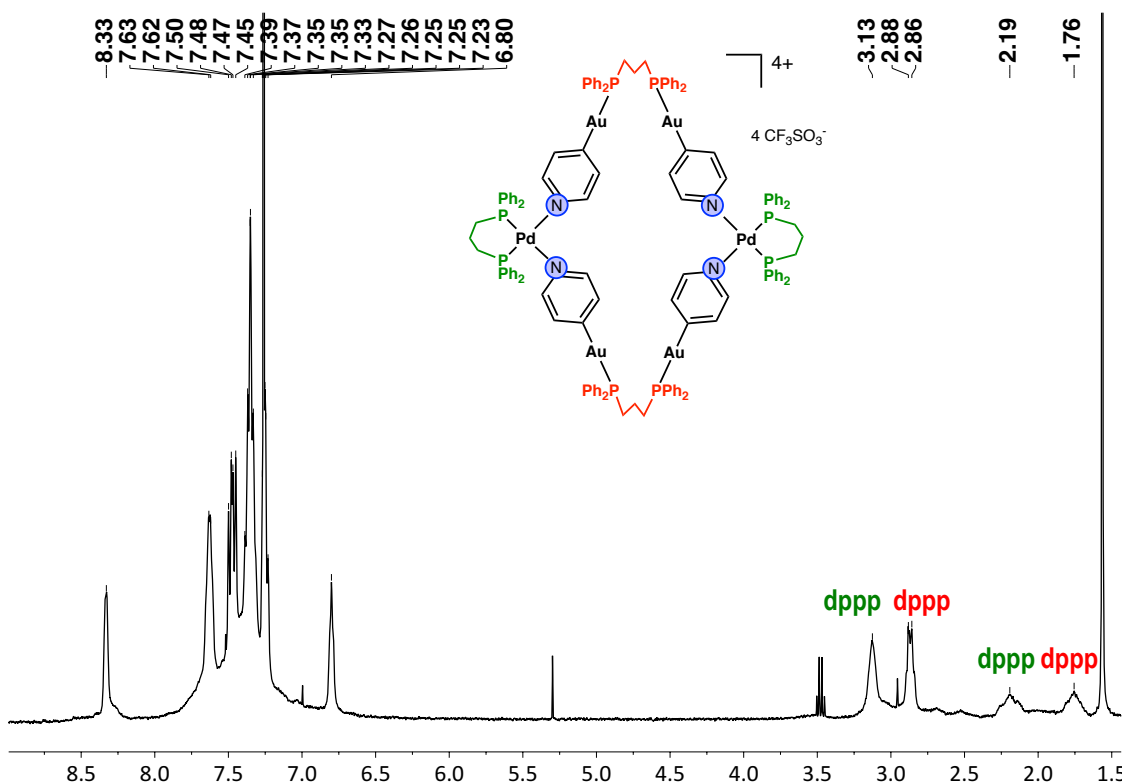


Figure S37. ^1H NMR of $\{(\text{Au4-py})_2(\mu_2\text{-dppp})\}_2\{\text{Pd}(\text{dppp})\}_2\{(\text{CF}_3\text{SO}_3)_4\}$ (**3₂A₂**) in CDCl_3 at 298 K.

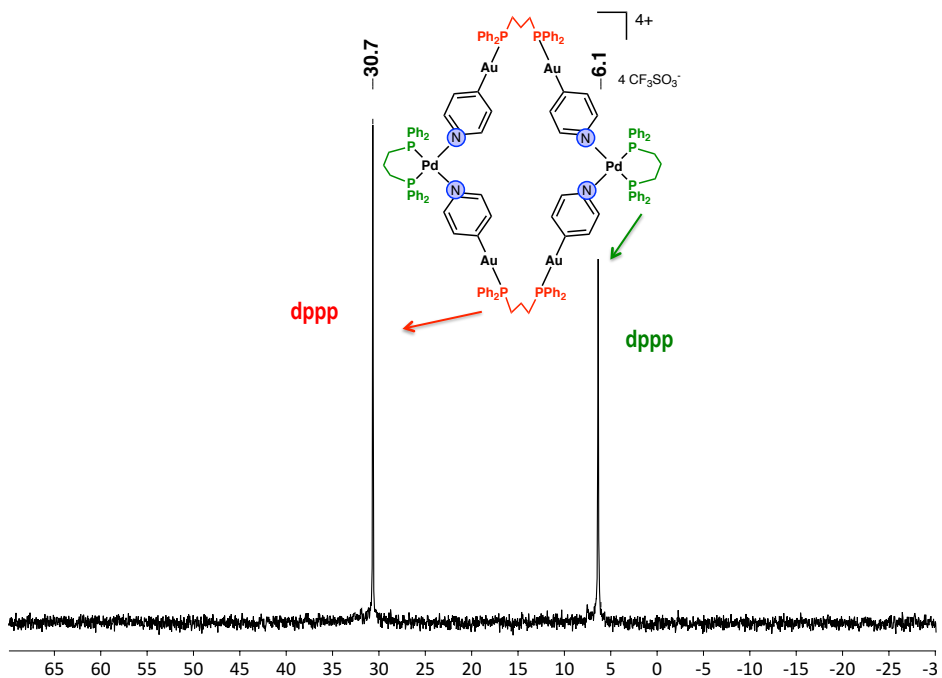


Figure S38. $^{31}\text{P}\{^1\text{H}\}$ NMR of $\{(\text{Au4-py})_2(\mu_2\text{-dppp})\}_2\{\text{Pd}(\text{dppp})\}_2\{(\text{CF}_3\text{SO}_3)_4\}$ (**3₂A₂**) in CDCl_3 at 298 K.

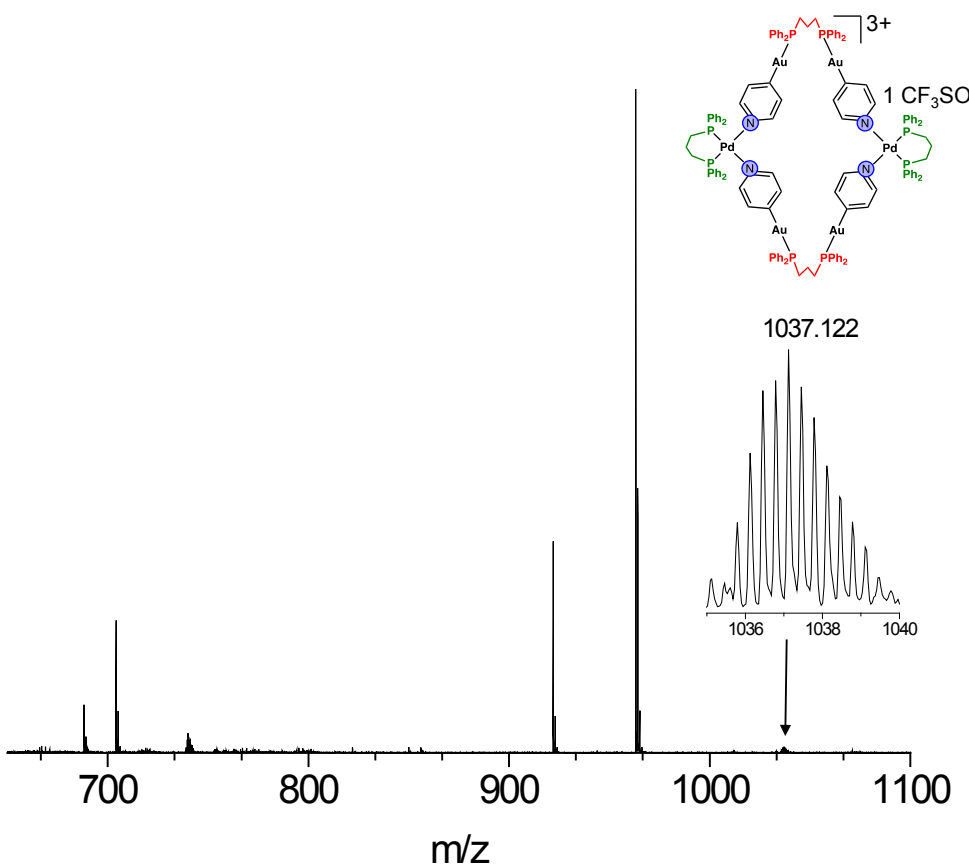


Figure S39. ESI(+) - HRMS spectrum of $\{(\text{Au4-py})_2(\mu_2\text{-dPPP})\}_2\{\text{Pd}(\text{dPPP})\}_2\text{[CF}_3\text{SO}_3\text{]}_4$ (**3₂A₂**).

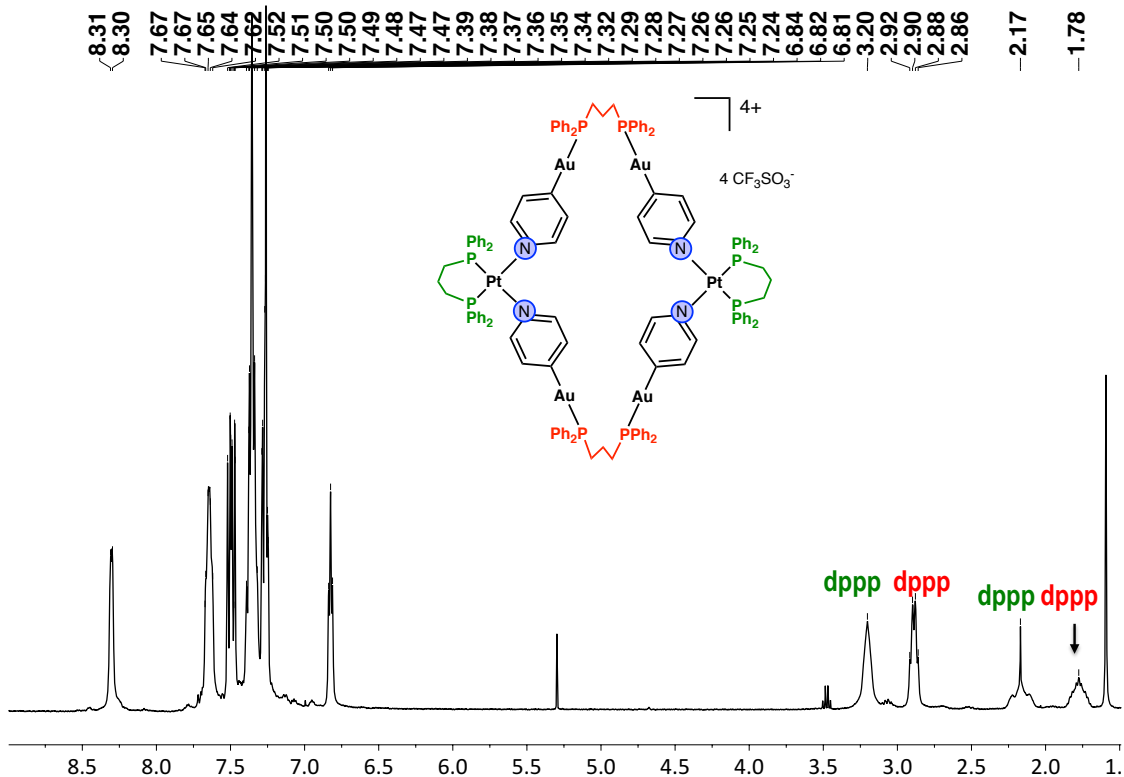


Figure S40. ^1H NMR of $\{(\text{Au4-py})_2(\mu_2\text{-dPPP})\}_2\{\text{Pt}(\text{dPPP})\}_2\text{[CF}_3\text{SO}_3\text{]}_4$ (**3₂B₂**) CDCl_3 at 298K.

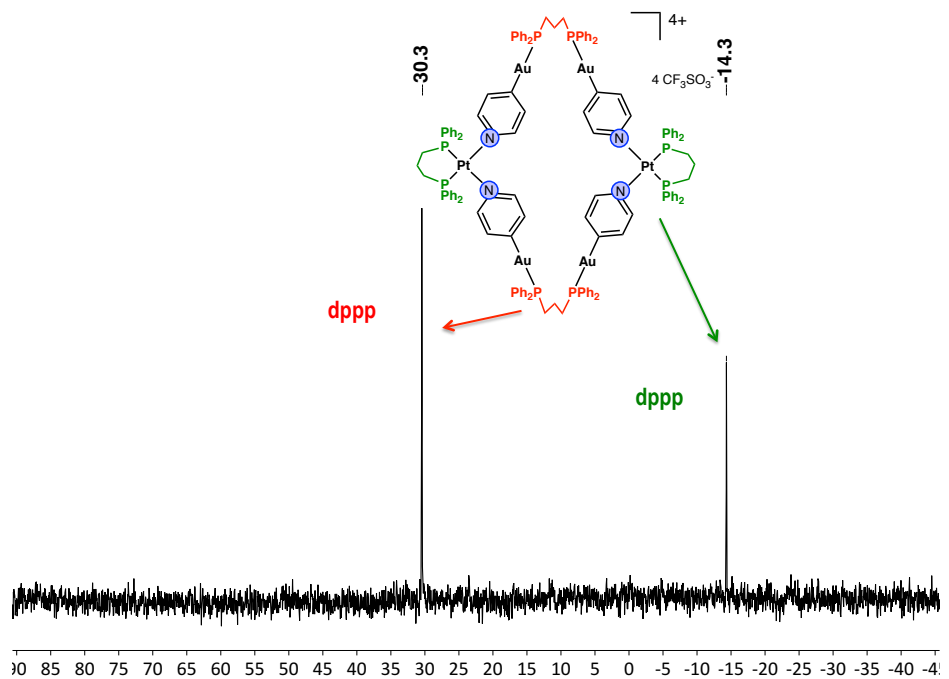


Figure S41. $^{31}\text{P}\{\text{H}\}$ NMR of $\{(\text{Au4-py})_2(\mu_2\text{-dPPP})\}_2\{\text{Pt}(\text{dPPP})\}_2](\text{CF}_3\text{SO}_3)_4$ (**3₂B₂**) in CDCl_3 at 298 K.

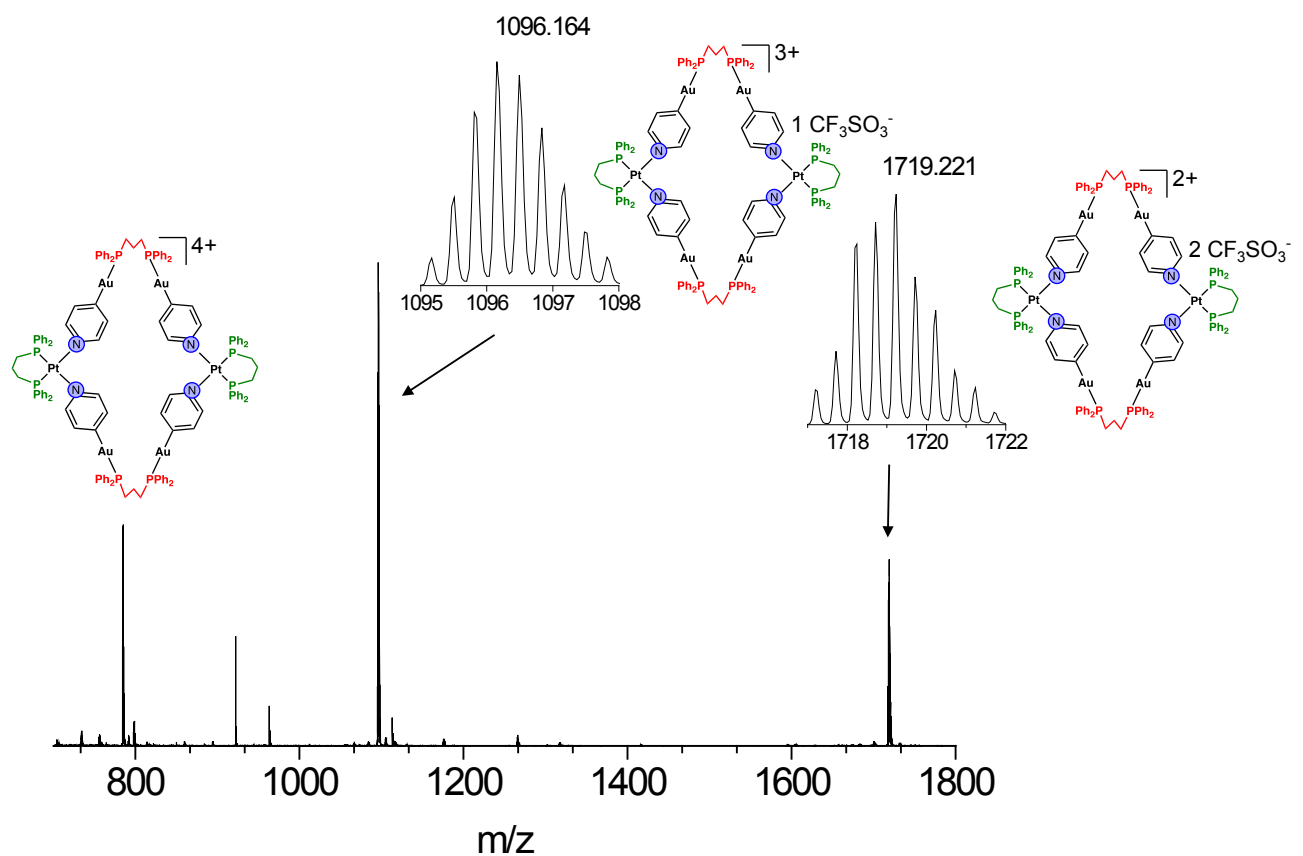


Figure S42. ESI(+)-HRMS spectrum of $\{(\text{Au4-py})_2(\mu_2\text{-dPPP})\}_2\{\text{Pt}(\text{dPPP})\}_2](\text{CF}_3\text{SO}_3)_4$ (**3₂B₂**).

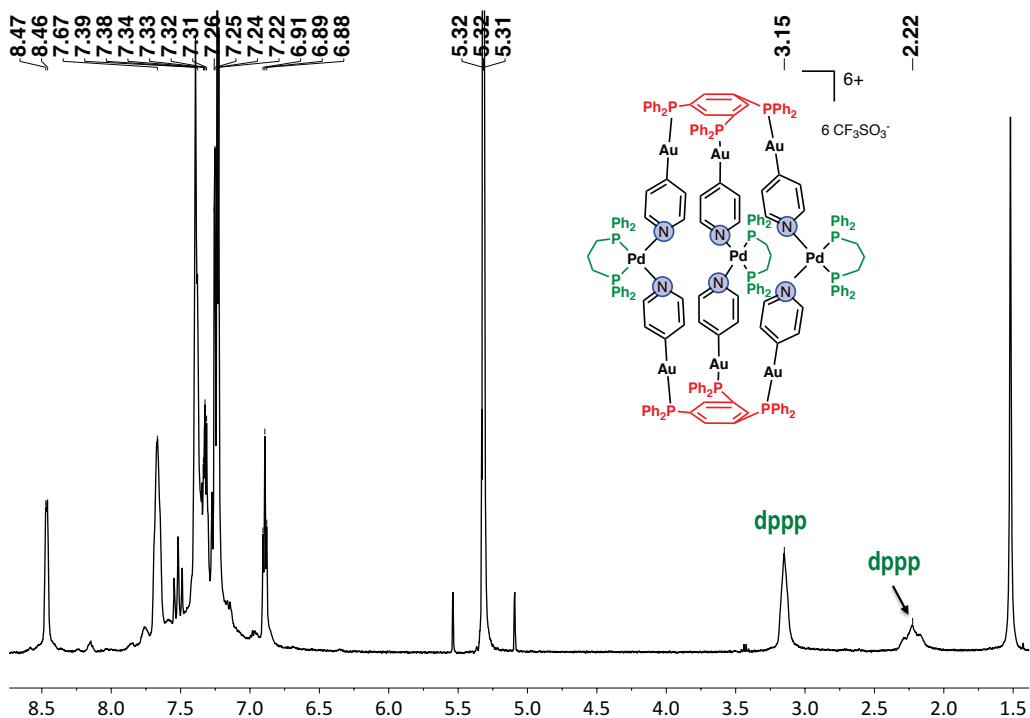


Figure S43. ^1H NMR of $\{(\text{Au4-py})_3(\mu_3\text{-triphasph})\}_2\{\text{Pd}(\text{dPPP})\}_3](\text{CF}_3\text{SO}_3)_6$ (**6₂A₃**) CD_2Cl_2 at 298 K.

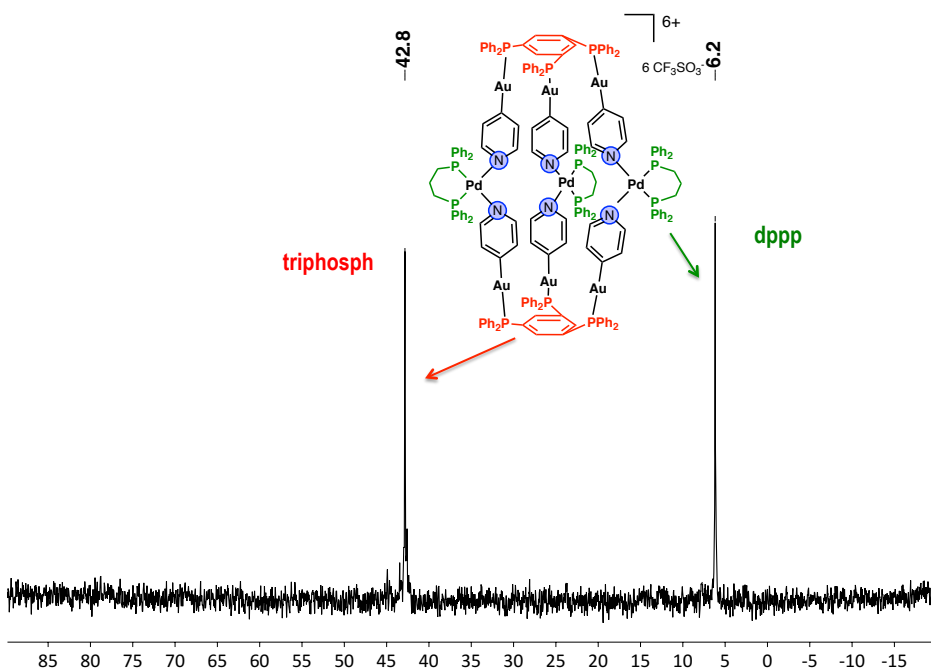


Figure S44. $^{31}\text{P}\{^1\text{H}\}$ NMR of $\{(\text{Au4-py})_3(\mu_3\text{-triphasph})\}_2\{\text{Pd}(\text{dPPP})\}_3](\text{CF}_3\text{SO}_3)_6$ (**6₂A₃**) CD_2Cl_2 at 298 K.

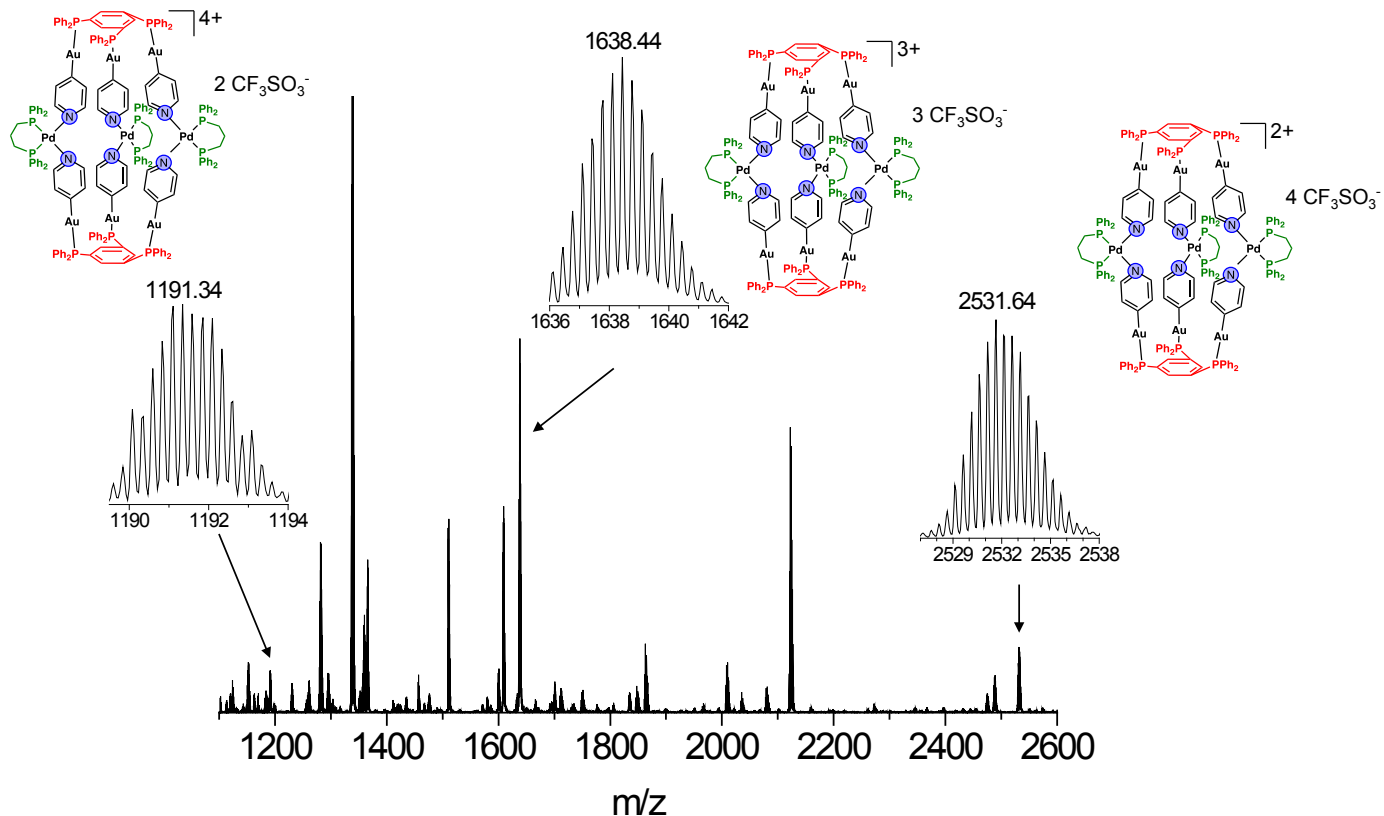


Figure S45. ESI(+) -HRMS spectrum of $\{(\text{Au4-py})_3(\mu_3\text{-triphospho})\}_2\{\text{Pd(dPPP)}\}_3\}(\text{CF}_3\text{SO}_3)_4$ ($\mathbf{6}_2\mathbf{A}_2$).

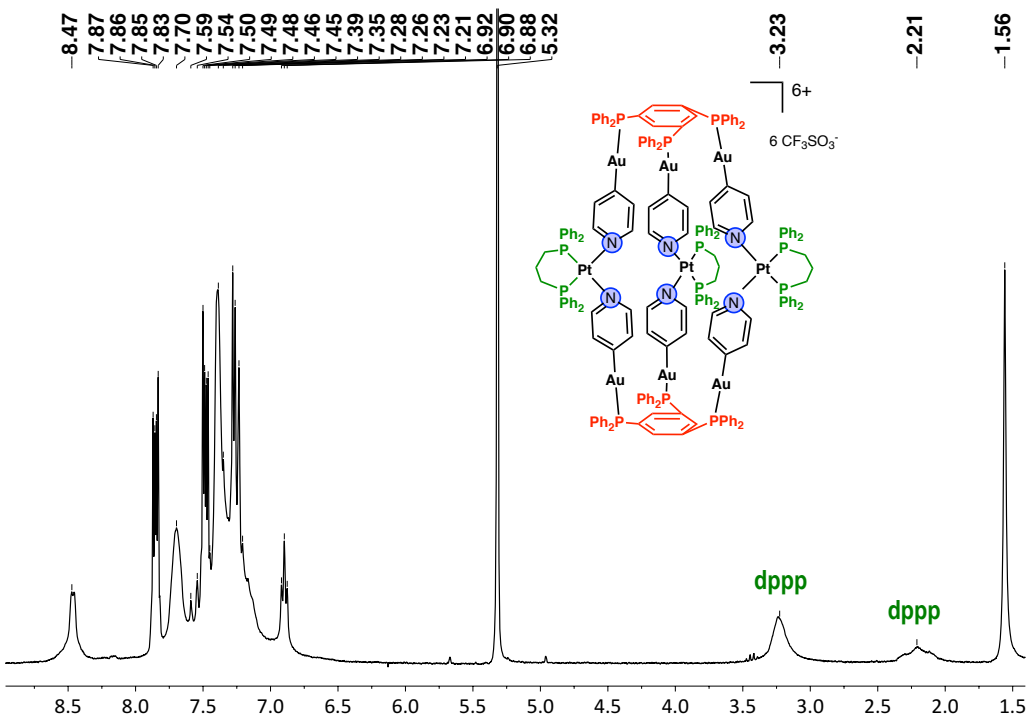


Figure S46. ^1H NMR of $\{(\text{Au4-py})_3(\mu_3\text{-triphospho})\}_2\{\text{Pt(dPPP)}\}_3\}(\text{CF}_3\text{SO}_3)_6$ ($\mathbf{6}_2\mathbf{B}_3$) in CD_2Cl_2 at 298 K.

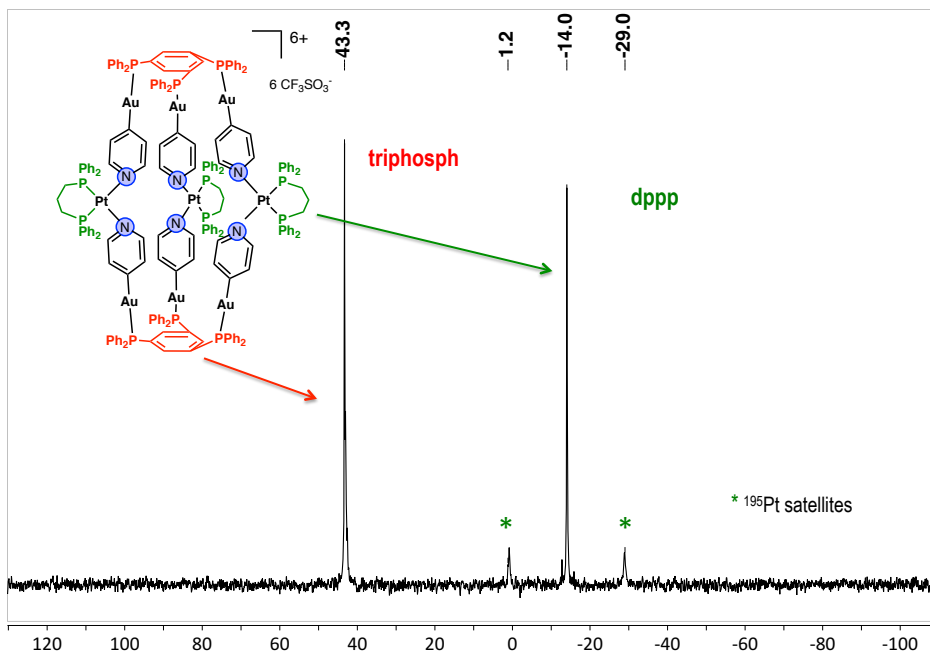


Figure S47. $^{31}\text{P}\{\text{H}\}$ NMR of $\{(\text{Au4-py})_3(\mu_3\text{-triphosph})\}_2\{\text{Pt(dppp)}\}_3](\text{CF}_3\text{SO}_3)_6$ (**6₂B₃**) in CD_2Cl_2 at 298 K.

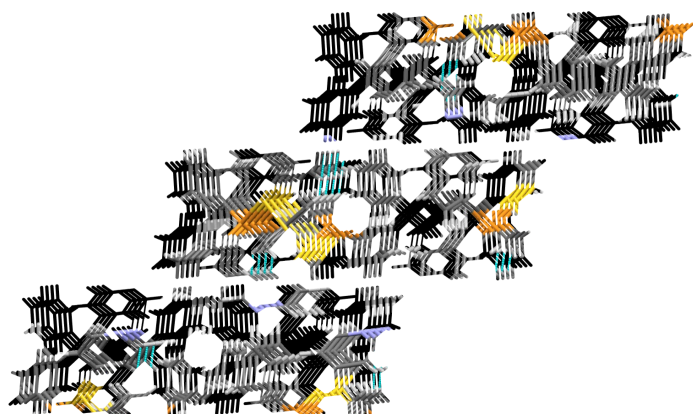


Figure S48. View of the molecular packing of compound **3** along the crystallographic *b*-axis. Weak C-H...π(ring) interactions between hydrogen atoms of the alkyl chain of the dppp and the pyridine rings of adjacent molecules are indicated in green colour.

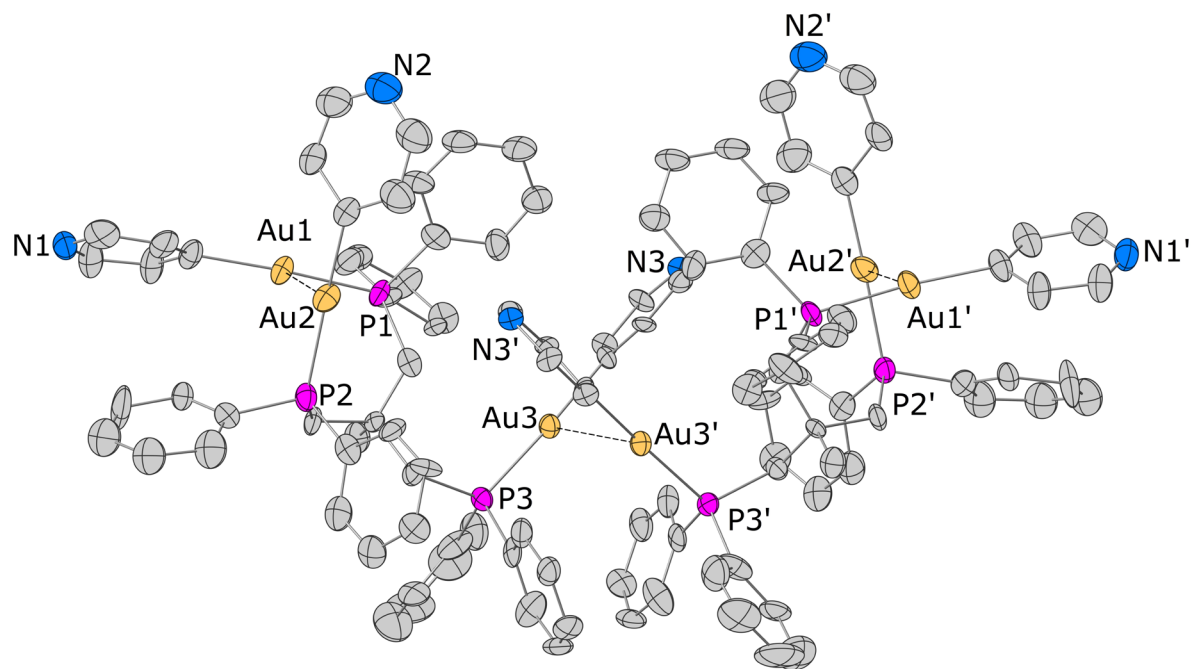


Figure S49. Representation of the dimeric structure of compound **5**.

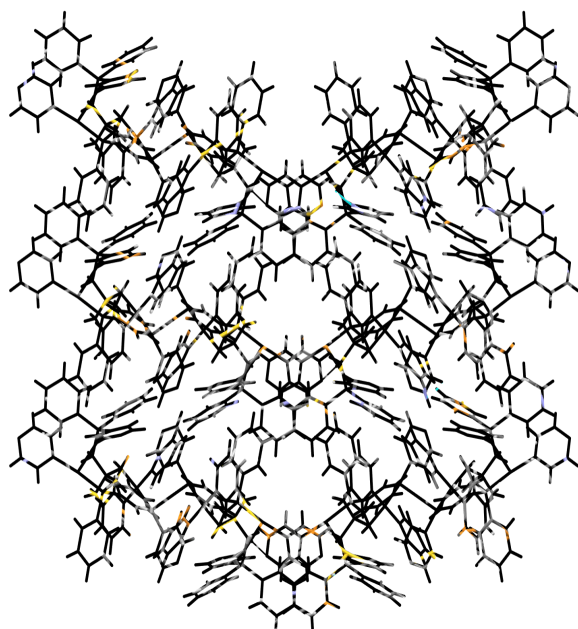


Figure S50. View of the molecular packing of compound **5** along the crystallographic *c*-axis. Weak C-H...N_{py} interactions between hydrogen atoms of the alkyl chain of triphos and the nitrogen atoms of pyridine rings of adjacent molecules are indicated in blue color.

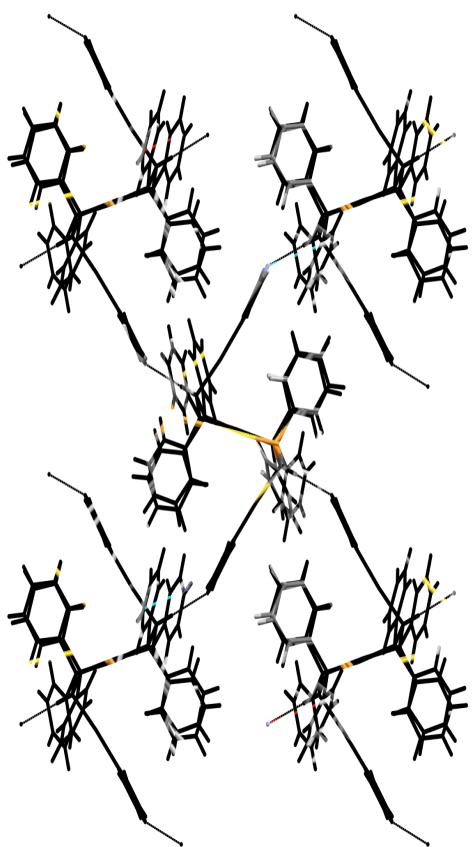


Figure S51. View of the molecular packing of compound **I** along the crystallographic *b*-axis. A layer structure is formed as a result of the establishment of C-H \cdots N_{py} contacts (in blue and red colors) between the molecules of compound **I**.

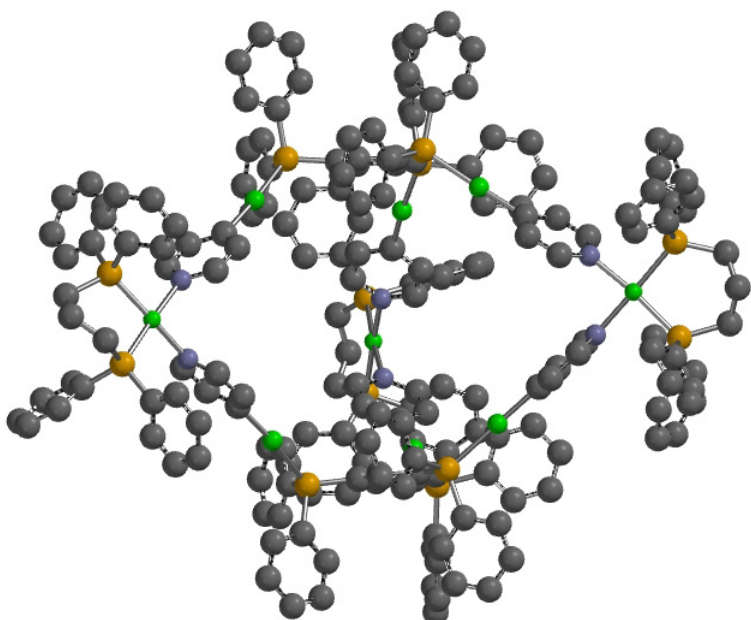


Figure S52. Ball and spoke model of the calculated structure (DFT-B3LYP) of [{(Au4-phenyl)₃}₃(μ₃-tripphospho)}₂{Pd(dPPP)}₃]⁶⁺ metallocage (**6A**₃ cation) (hydrogens are omitted for clarity).

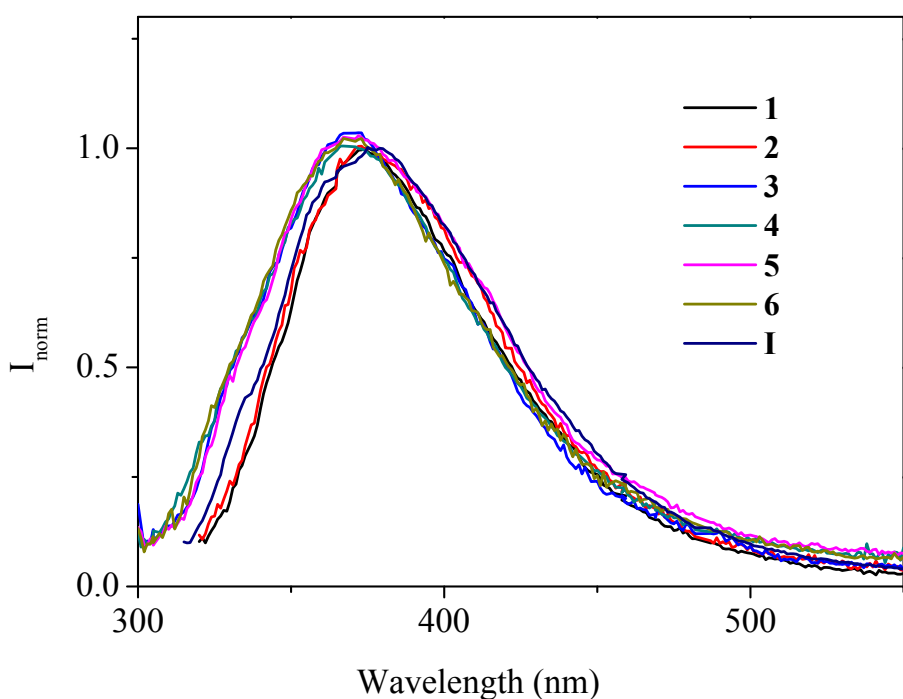
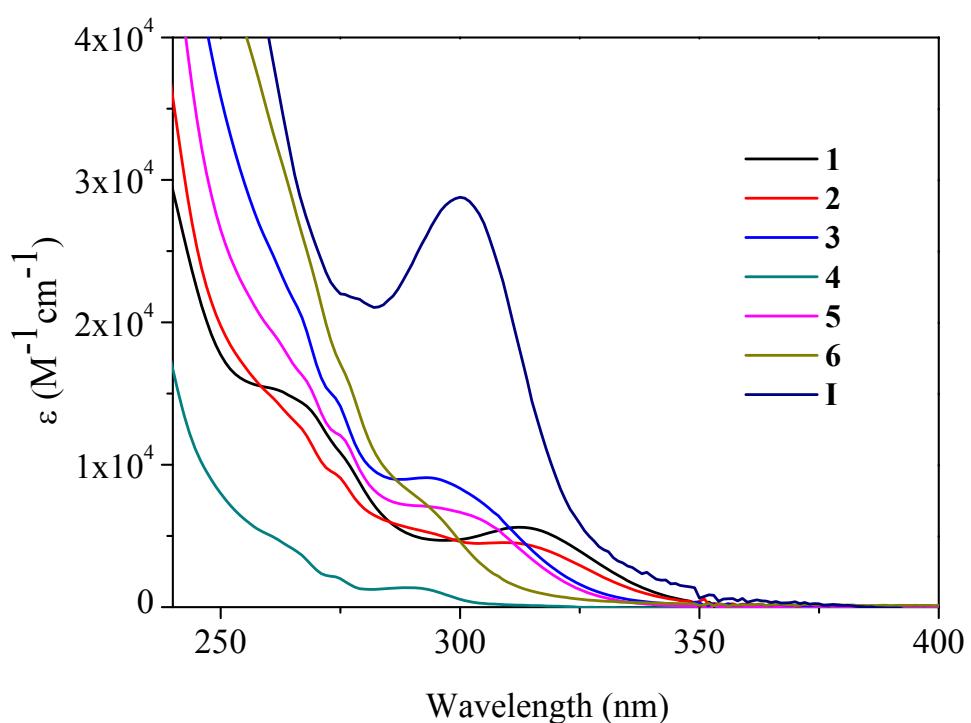


Figure S53. Absorption (above) and normalized emission (below) spectra of metallaligands **1-6** and **I**.

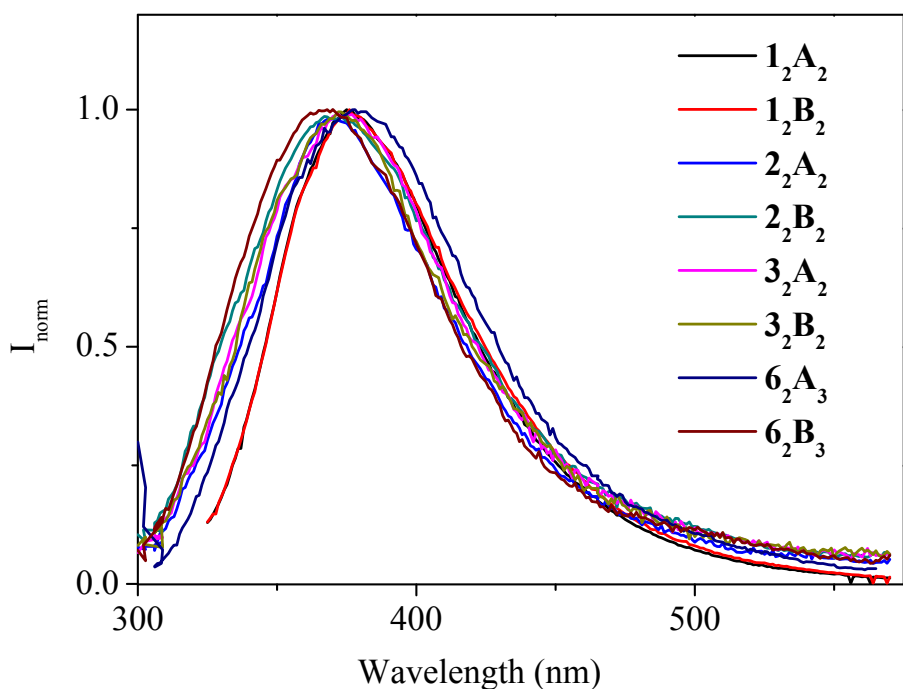
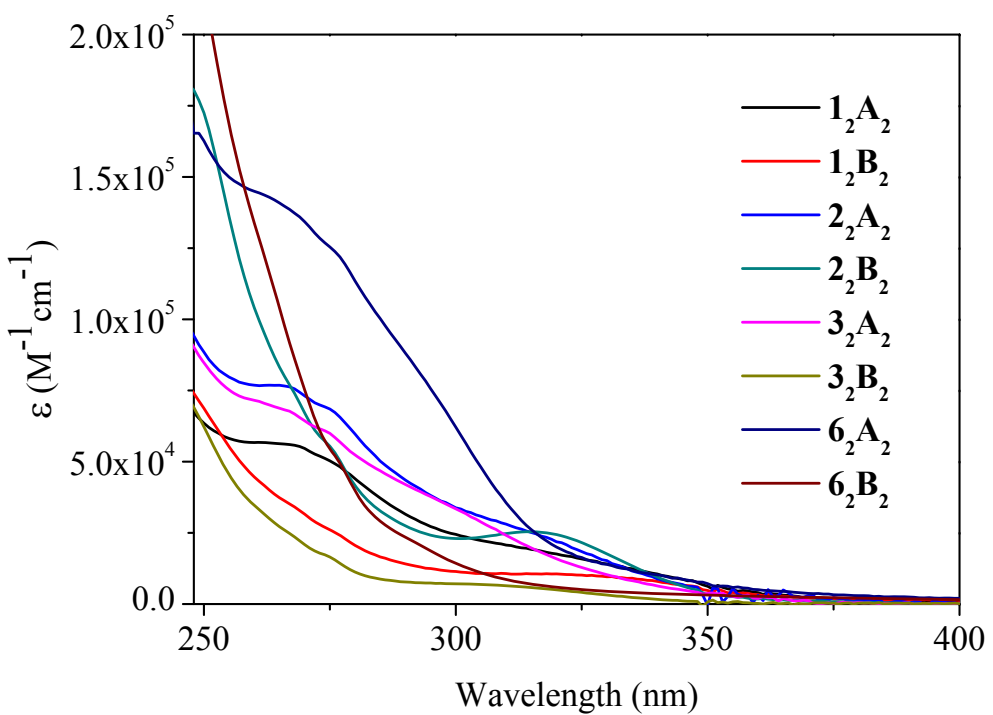


Figure S54. Absorption (above) and normalized emission (below) spectra of metallamacrocycles and metallacages.

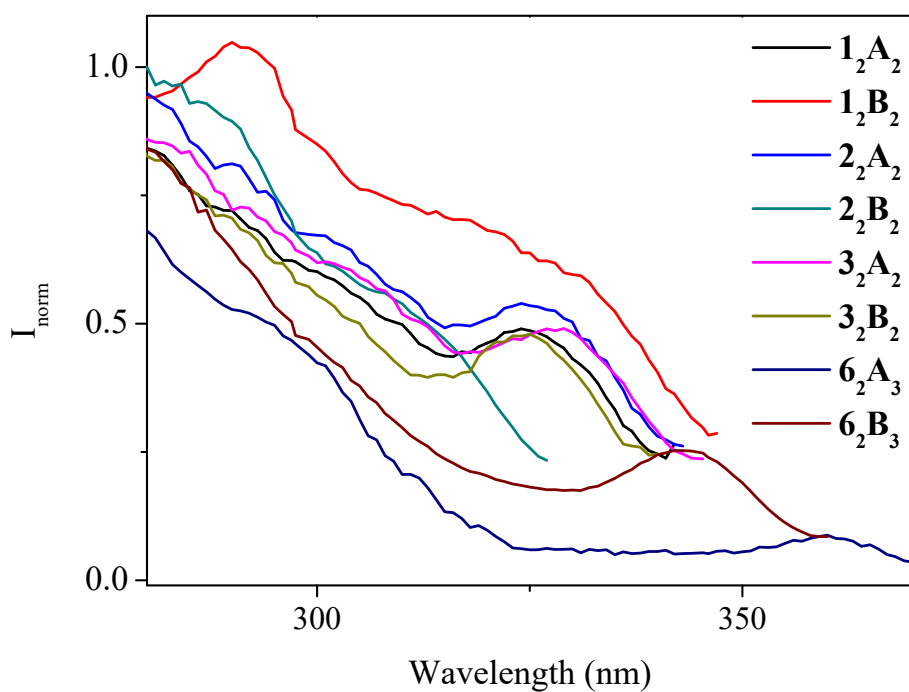


Figure S55. Excitation spectra of the metallamacrocycles collected at the emission maxima.

Crystal data

Crystal data for **1**: M = 1965.54, plate, 0.16 x 0.13 x 0.06 mm³, orthorhombic, space group *Pbca*, $a = 19.30536(10)$ Å, $b = 21.42084(10)$ Å, $c = 30.38661(15)$ Å, $\alpha = 90^\circ$, $\beta = 90^\circ$, $\gamma = 90^\circ$, V = 12565.99(11) Å³, Z = 8, D_c = 2.078 g/cm³, F000 = 7408, $\mu = 20.793$ mm⁻¹, T = 123.0 K, θ range for data collection = 2.908 to 66.740°, 11124 reflections with 10785 [$I_o > 2\sigma(I_o)$], R_{int} = 0.0307, reflections/parameters/restraints = 11124/712/12, GoF = 1.117, R = 0.0270 and wR = 0.0639 [$I_o > 2\sigma(I_o)$], R = 0.0282 and wR = 0.0646 (all reflections), -1.592 < ΔQ < 1.238 e/Å³. CCDC-2000611 contains the supplementary crystallographic data for this paper. These data can be obtained free of charge from The Cambridge Crystallographic Data Centre via www.ccdc.cam.ac.uk/data_request/cif

Crystal data for **2**: M = 948.51, plate, 0.4639 x 0.2693 x 0.0402 mm³, monoclinic, space group *C2/c*, $a = 16.5827(3)$ Å, $b = 9.97851(17)$ Å, $c = 19.3563(3)$ Å, $\alpha = 90^\circ$, $\beta = 104.6607(18)^\circ$, $\gamma = 90^\circ$, V = 3098.62(10) Å³, Z = 4, D_c = 2.033 g/cm³, F000 = 1800, $\mu = 18.739$ mm⁻¹, T = 123.0 K, θ range for data collection = 4.723 to 67.684°, 5383 reflections with 2827 independent and 2758 [$I_o > 2\sigma(I_o)$], R_{int} = 0.0380, reflections/parameters/restraints = 2827/190/0, GoF = 1.138, R = 0.0376 and wR = 0.1045 [$I_o > 2\sigma(I_o)$], R = 0.0376 and wR = 0.1052 (all reflections), -3.751 < ΔQ < 2.637 e/Å³. CCDC-2000612 contains the supplementary crystallographic data for this paper. These data can be obtained free of charge from The Cambridge Crystallographic Data Centre via www.ccdc.cam.ac.uk/data_request/cif

Crystal data for **3**: M = 962.54, block, 0.1104 x 0.0672 x 0.0415 mm³, monoclinic, space group *C2/c*, $a = 25.7663(6)$ Å, $b = 7.6243(10)$ Å, $c = 22.7420(3)$ Å, $\alpha = 90^\circ$, $\beta = 134.2170(10)^\circ$, $\gamma = 90^\circ$, V = 3201.99(10) Å³, Z = 4, D_c = 1.997 g/cm³, F000 = 1832, $\mu = 18.146$ mm⁻¹, T = 123.0 K, θ range for data collection = 3.9890 to 75.5610°, 6508 reflections with 3290 independent and 3207 [$I_o > 2\sigma(I_o)$], R_{int} = 0.0162, reflections/parameters/restraints = 3290/195/0, GoF = 1.113, R = 0.0210 and wR = 0.0557 [$I_o > 2\sigma(I_o)$], R = 0.0216 and wR = 0.0562 (all reflections), -1.314 < ΔQ < 0.667 e/Å³. CCDC-2000613 contains the supplementary crystallographic data for this paper. These data can be obtained free of charge from The Cambridge Crystallographic Data Centre via www.ccdc.cam.ac.uk/data_request/cif

Crystal data for **5**: M = 1449.80, needle, 0.486 x 0.0363 x 0.0236 mm³, orthorhombic, space group *Aea2*, $a = 36.6920(7)$ Å, $b = 21.4267(5)$ Å, $c = 13.8250(3)$ Å, $\alpha = 90^\circ$, $\beta = 0^\circ$, $\gamma = 90^\circ$, V = 10869.0(4) Å³, Z = 8, D_c = 1.772 g/cm³, F000 = 5520, $\mu = 16.040$ mm⁻¹, T = 123.0 K, θ range for data collection = 3.9740 to 75.3050°, 22013 reflections with 8487 independent and 7928 [$I_o > 2\sigma(I_o)$], R_{int} = 0.0363, reflections/parameters/restraints = 8487/587/115, GoF = 1.206, R = 0.0660 and wR = 0.1754 [$I_o > 2\sigma(I_o)$], R = 0.0693 and wR = 0.1768 (all reflections), -2.355 < ΔQ < 3.761 e/Å³. CCDC-2000614 contains the supplementary crystallographic data for this paper. These data can be obtained free of charge from The Cambridge Crystallographic Data Centre via www.ccdc.cam.ac.uk/data_request/cif